Attenuation Correction Techniques in Nuclear Medicine - SPECT, PET

Rahul P. Mahajan
Research and Development Department, Healthcare and Medical Device Development Industry
College of Engineering, Pune, India
rpm.mahajan@gmail.com

0009-0003-3038-4391

***Abstract*—**In contemporary clinical practice, Anatomical imaging modalities are improved by nuclear medicine imaging, which provides molecular and functional insights. Nuclear medicine imaging has emerged as a crucial tool in modern clinical practice, providing molecular and functional insights that improve anatomical imaging modalities. Among its often-used methods, single-photon emission computed tomography (SPECT) and positron emission tomography (PET) are essential for the diagnosis, staging, and follow-up of a wide range of illnesses, such as neurological, cardiovascular, and cancer conditions. However, photon attenuation has a major impact on the precision and clinical usefulness of PET and SPECT, a phenomenon in which photons are absorbed or scattered by tissues before reaching the detector. Attenuation leads to image degradation, artefacts, and errors in tracer quantification, ultimately affecting diagnostic precision and treatment planning. This study presents a thorough analysis of nuclear medicine imaging attenuation correction strategies, emphasizing both conventional and modern approaches. Foundational approaches such as uniform attenuation maps, Chang's algorithm, and iterative reconstruction are discussed alongside the revolutionary contributions of hybrid imaging techniques that combine anatomical data to produce precise attenuation maps, such as PET/CT, SPECT/CT, and PET/MR. Additionally, the potential of developments in artificial intelligence (AI), such as deep learning (DL) and machine learning (ML) to enhance image reconstruction, automate attenuation correction, and simplify workflow. Clinical applications across cardiology, oncology, neurology, musculoskeletal imaging, and infection detection are highlighted to demonstrate the impact of accurate attenuation correction in improving diagnostic confidence and patient outcomes. By tracing the evolution of techniques and highlighting recent innovations, this paper underscores the central role of attenuation correction in maximizing the diagnostic and therapeutic potential of nuclear medicine imaging.

Keywords*—Nuclear Medicine, Attenuation Correction, PET, SPECT, Photon Attenuation, Scatter Correction, Clinical Applications, Quantitative Imaging.*

I. INTRODUCTION

In modern healthcare, nuclear medicine imaging (NMI) is a crucial technique for medical diagnosis and treatment that uses a small, regulated amount of radio diagnostic reagents. The purpose of the reagents is to attach themselves to chemical carriers that either accumulate through various physiological routes associated with neoplasia or move to specific regions of it. This makes it possible to treat patients with greater precision [1]. Alpha, gamma, and beta radiation-releasing radiopharmaceuticals are on a list that authorized by the US Food and Drug Administration. Nuclear medicine imaging makes use of a variety of radioisotope sensing techniques. These consist of single-photon emission-computed tomography (SPECT), positron emission tomography (PET), scintigraphy, and planar imaging.

However, both SPECT and PET face a critical challenge in the form of attenuation, a major physical degrading factor in nuclear medicine imaging, which occurs when photons emitted from radiopharmaceuticals are absorbed or scattered by surrounding tissues before reaching the detector. This effect leads to underestimation of tracer uptake in deeper structures, reduced image contrast, and possible misdiagnosis. To address this challenge, attenuation correction (AC) techniques have been developed for both SPECT and PET imaging. Reliable quantitative analysis is made possible by the creation of precise attenuation maps in PET through the use of combined CT images [2]. In SPECT, however, attenuation correction is more complex due to photon energy variability and the absence of standardized correction methods, though CT-based, transmission-based, and advanced algorithmic approaches are increasingly applied. The incorporation of AC significantly

enhances image uniformity, diagnostic accuracy, and clinical confidence by ensuring that reconstructed images more faithfully represent physiological activity rather than artifacts caused by tissue absorption.

Recent developments in technology are making SPECT/CT a more competitive diagnostic imaging method [3]. These developments cover both the hardware and software used for data gathering. The former allows for improved processing of projection data to generate images of superior quality, which facilitates the measurement of clinically important factors and image analysis. As SPECT and SPECT/CT systems have advanced, more sensitive detector materials have been developed, leading to the replacement of scintillator NaI (Tl) detectors with semiconductor detectors. Another noteworthy development is the widespread use of signal amplifier devices like silicon photomultiplier tubes (SiPMs), avalanche photodiodes (APDs), and position-sensitive photomultiplier tubes (PSPMTs) in place of traditional photomultiplier tubes (PMTs). The performance of single-purpose and multi-purpose SPECT and SPECT/CT systems has been enhanced by innovative collimator and camera head designs [4]. To take use of the new hardware technologies' high photon-counting capabilities, SPECT and SPECT/CT imaging software approaches have to be developed. The most evident developments in software approaches are the use and commercial availability of quantitative methodologies, data rectification procedures, and reconstruction algorithms.

By overcoming these physical constraints, NMI, which entails visualizing organ functions offers comprehensive and useful insights for neurological disorders, cancer detection, respiration/perfusion scanning, bone scintigraphy, thyroid radioiodine scanning, renal scintigraphy, liver and spleen scintigraphy, and cardiovascular monitoring. Medical professionals and professional technicians have had to devote a significant amount of time and resources to processing and training since large data management and the creation of diagnostic tools for modern healthcare have advanced so quickly over the past few decades [5][6], activities that would not be feasible without the application of ever-more-innovative and complicated algorithms. In many applications, the advancement of deep learning (DL) has produced impressive results and shown capabilities that are superior to those of humans. DL algorithms may be created using pipeline-designed procedures to take use of all available data using methods including segmentation, anomaly detection, computer-aided diagnostics, and denoising to enhance the image quality.

Additionally, Hybrid imaging systems such as PET/CT and SPECT/CT combine anatomical and functional data in a single scan, combined with sophisticated computational techniques, have transformed nuclear medicine. This synergy not only enhances attenuation correction but also improves localization of lesions and disease characterization [7]. Recent innovations in artificial intelligence (AI) and DL have further expanded these capabilities by enabling automated attenuation map generation, artifact reduction, and quantitative image analysis, even in scenarios where CT data are unavailable. Such advancements pave the way for precision diagnostics and personalized treatment planning, ensuring that nuclear medicine imaging evolves beyond conventional visualization toward a data-driven, patient-centered approach.

A. Structure of the Paper

The paper is structured as follows: Section II introduces medical imaging. Section III covers attenuation correction and Section IV covers early developments, while Section V explains attenuation fundamentals in nuclear medicine. Section VI discusses hybrid imaging, followed by Section VII, comparing PET and SPECT. Section VIII highlights AI in SPECT/SPECT-CT, and Section IX addresses clinical implications of recent advances. Section X details PET and SPECT technology, Section XI covers PET radionuclides, Section XII explains SPECT principles and radiopharmaceuticals, and Section XIII presents SPECT applications. Section XIV reviews literature, and Section XV concludes with future directions.

II. Overview of Medical Imaging

Medical imaging may be a common and necessary component of medicine in any setting where processing applications are utilized to help radiologists and clinicians with their everyday tasks. Computer-aided pathology diagnosis, computer-aided image registration, treatment planning and guidance, and disease progression tracking are just a few of the uses for data gleaned from medical images [8]. This field's main benefit is that health issues may actually be viewed rather than inferred from symptoms. Examples of health problems include fractures, brain anomalies, as well as breast and prostate malignancies. The crucial

or dangerous health-related problem is to detect malignancy or abnormalities in any part of the patient's body.

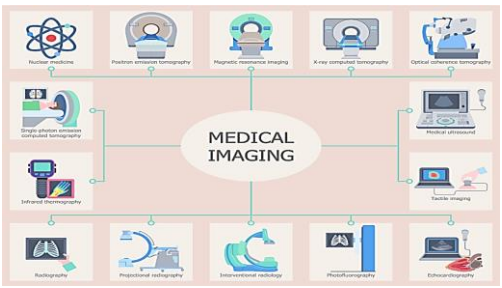

Fig. 1. Medical Imaging

The several medical imaging modalities used for diagnosis and therapy planning are summarized in Figure 1. It emphasizes nuclear medicine, PET, MRI, CT, and other structural and functional imaging methods, and optical coherence tomography, which visualize internal anatomy and physiological processes. Medical ultrasonography, tactile imaging, and SPECT are further modalities, and infrared thermography, offer additional functional or surface-level insights. Conventional X-ray–based methods, like radiography, projectional radiography, interventional radiology, and photofluorography, focus on anatomical imaging, while echocardiography specifically assesses cardiac function. Collectively, these imaging technologies provide clinicians with a comprehensive toolkit for accurate diagnosis, monitoring, and guiding therapeutic interventions.

A. Basic Concept of Medical Image

An array of image elements, known as pixels or voxels that depict the internal structure or function of an atomic area is known as a medical image. It is a discrete representation that links numerical values to spatial locations as a result of sampling and reconstruction. A precise acquisition modality's field-of-view is described by the number of pixels [9][10]. The pixel values' numerical values convey the reliance on the imaging modality, acquisition methodology, reconstruction, and, ultimately, postprocessing. A basic overview of medical image modalities and their operation is given in the next section.

B. Medical Imaging

Medical imaging is used to see bodily organs, tissues, or components. This helps with clinical diagnosis, treatment, and sickness tracking. Imaging methods include optical imaging, nuclear medicine, and radiology.

- **Radiology:** This technique offers extremely high spatial and temporal resolution of the human body's anatomy and physiology. This field includes techniques such as MRI, CT, X-ray, and ultrasound [8]. Contrast agents can be used to improve these images.
- **Nuclear Medicine:** Nuclear imaging methods like PET and SPECT employ radioactive tracers to provide remarkably detailed information about the body's physiology, metabolism, and molecular activity.
- **Optical Imaging:** The majority of hollow organs' structural and functional data may be shown in real time at the cellular level using optical imaging methods like optical coherence tomography (OCT). High-resolution images, such those produced by optical tracers that are particular to tumor cells, indicate the anomalies. The development of this method is still in its infancy.

C. Medical Imaging Modalities

In an ideal world, assist in identifying patients and cure them without having harmful side effects. One of the greatest methods to accomplish that goal is still through Medical imaging, which eliminates the need for intrusive operations like surgery and lets one observe what's happening within the body. Because it may be used for both diagnosis and therapy, it is one of the most effective instruments for giving patients the care they need [11]. Imaging modalities such as X-rays, CT, MRI, and PET are commonly employed in the diagnostic process. They all use somewhat different methods to provide images of the human body's inside. The details of each medical modality are mentioned below.

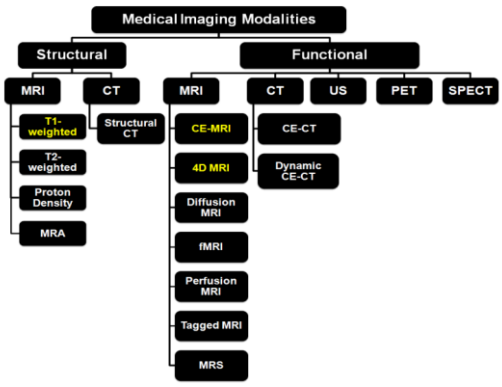

Fig. 2. Categories of Medical Image Modalities

According to the type of information they provide, structural or functional imaging about the organ being imaging, for example, Figure 2 lists the categories of medical imaging modalities. The following methods are represented by the acronyms: PET, CT, positron emission tomography, computed tomography, single photon emission computed tomography, functional magnetic resonance imaging, contrast-enhanced magnetic resonance imaging, and MRI in general. This dissertation mostly addresses the yellow-coloured groups.

1) X-RAY

A kind of electromagnetic radiation, it resembles light in appearance. It has a greater energy and can pierce most materials, even flesh [12]. To provide photographs of the inside of human tissues and structures, X-rays are utilized in medicine. When X-rays move through the body and pass through an X-ray detector on the other side of the patient, a picture is created that depicts the "shadows" cast by internal things.

Although there are several varieties of x-ray detectors, imaging film is one type. To create digital images, these detectors are employed. This process creates radiographs, which are x-ray images.

a) Working of X-Ray

The process of creating a radiograph begins with positioning the patient such that the area of the body being scanned is in the precise center of an x-ray detector and source (Figure 3). The equipment sends x-rays through the body when it is turned on, where their absorption changes based on the radiological density of the tissues they go through [13]. To get a substance's radiological density, one can compute the density of the material as well as the atomic number, or the quantity of protons in an atom's nucleus.

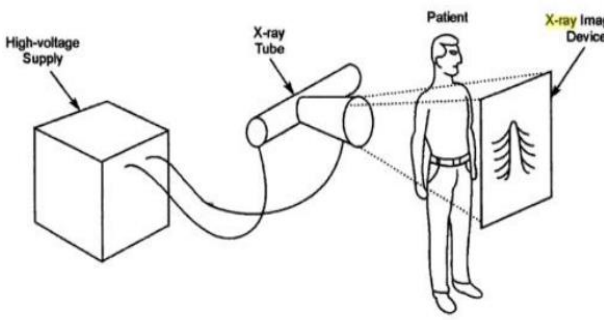

Fig. 3. The use of X-Ray to Visualize the Inner Structure of the Body

The block diagram of the central component of the X-ray apparatus, the X-ray generator, is seen in Figure 3. The X-ray tube in an X-ray generator produces the X-rays by bombardment of an anode target with fast-moving electrons obtained from a cathode [14]. The characteristic of X-ray beam depends on the anode-cathode voltage and the temperature of the electron-emitting cathode. For medical applications, particularly in diagnostic procedures, only a short burst of X-ray is used. A longer duration of radiation may be required for screening and therapy.

b) Diagnostic

In order to detect dental problems, aberrant masses, calcifications, pneumonia, bone fractures, specific tumors, X-ray radiography is frequently utilized.

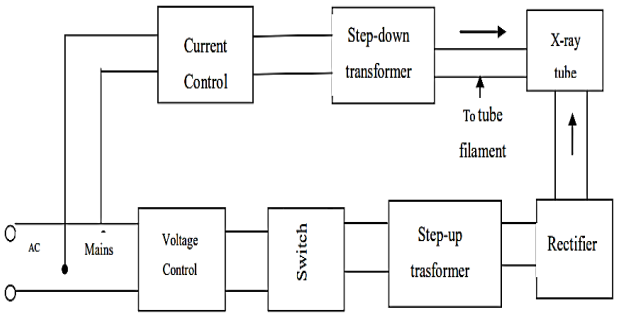

Fig. 4. The Block Diagram of an X-ray Generator

Figure 4 shows the basic working of an X-ray machine. AC mains power is regulated by voltage and current control units, then passed through a switch. A step-up transformer increases the X-ray tube's voltage, while a step-down transformer supplies current to the tube filament. For the X-ray tube to generate imaging-quality X-rays, the rectifier must first convert AC to DCs.

2) CT

The main drawback of conventional X-rays is that they overlay three-dimensional information on a single plane, which makes diagnosis confusing and often difficult. Second, because photographic film has a restricted dynamic range, objects with notable differences in X-ray absorption relative to their environment produce a contrast difference in the film that is perceptible to the naked eye.

a) Working of CT

The patient is transported inside the rigid gantry's aperture while lying on a motorized sofa. In this gantry, the detectors and X-ray source are placed across from

each other. One or both of these can be moved throughout the pertinent parts, measurements are taken [15]. A typical CT scan takes series of 2D axial slices of the patient which can be stacked to tube filament Voltage Control Switch Step-up transformer Rectifier X-ray tube Step-down transformer Current Control AC Mains 7 to form a 3D representation.

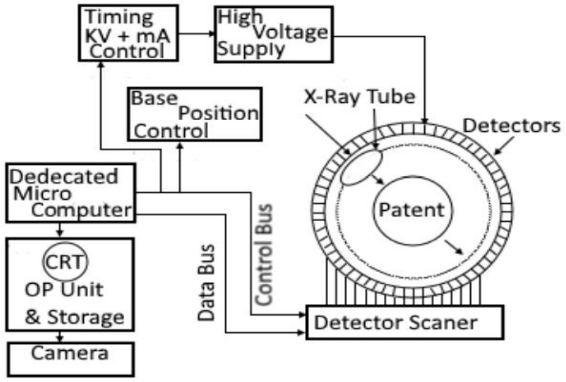

Fig. 5. Operation of CT Scanner

There are mainly two parts in CT imaging process namely slice data acquisition and slice reconstruction. In the former case, x-ray beam gets activated and rays spreads out which enters the human body at a plane required capturing image slice in Figure 5. With the progress of X ray power passing through the patient body, it generates tendency to pass through tissues [16]. Complete focus of ray power is considered through the edge of the tissue densities. And subsequent to the departure of ray through the human body, linear tissue density results are derived from the sensor array measurement. All such measurement data are captured and stored in digital form in computer.

b) Diagnostic

The CT scan modality is commonly employed for imaging of the chest and lungs, bone damage, and cancer detection.

3) MRI

The imaging method referred to as magnetic resonance imaging (MRI), produces practical diagnostic images by using non-ionizing radiation. Nuclear Magnetic Resonance Imaging was its original name [17]. The greatest places for MRI scans to image the body, which are tissues that are not skeletal. They don't utilize x-rays, which might cause harm, like computed tomography (CT) does. Compared to regular x-rays and CT scans, magnetic resonance imaging (MRI) provides a tremendously clearer image of the brain, spinal cord, nerves, ligaments, and tendons. Because of this, knee and shoulder injuries are commonly visualized using MRI.

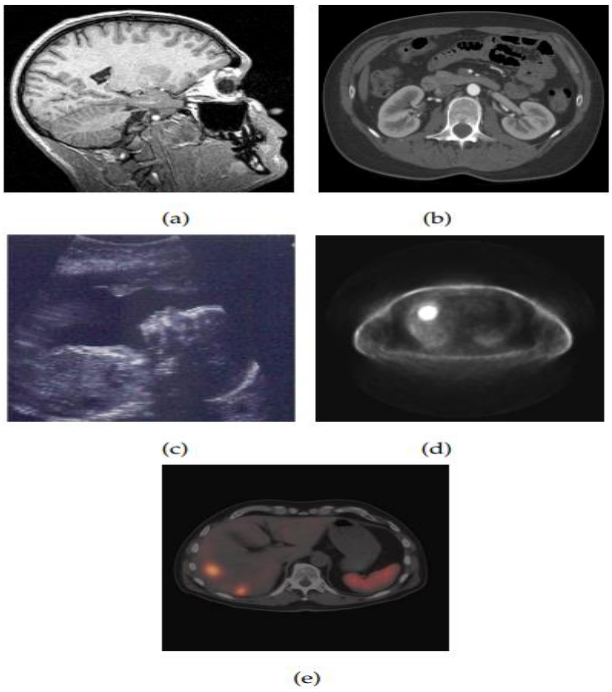

Fig. 6. Different Types of Medical Images

Figure 6 illustrates the many forms of medical imaging: (a) magnetic resonance imaging (MRI) of the brain, (b) computed tomography (CT) image of the kidney, (c) ultrasound (US) image of the fetus, (d) positron emission tomography (PET) image of the lung, and (e) single photon emission computed tomography (SPECT) image of the liver.

a) Working of MRI

The majority of the human body is composed of molecules of water, which are made up of hydrogen and oxygen atoms, the mechanisms and workings of MRI machines are grounded on the very principles of nuclear technology [18]. An even smaller particle named proton, is at each hydrogen atoms center. Protons resemble tiny magnets and are very sensitive to magnetic fields.

b) Diagnostic

The brain and other internal organs may be examined with MRI. It may also be used to identify the presence of certain illnesses and diagnose sports injuries. It is appropriate for evaluating soft tissues, such as brain tumors, injuries to ligaments and tendons, spinal cord injuries, etc.

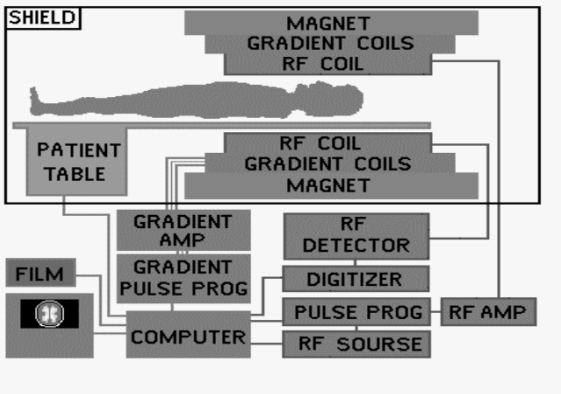

Fig. 7. The Block Diagram of MRI Scanner

Figure 7 shows the working of an MRI system, where the patient lies on a table inside a shielded magnet with gradient and RF coils. RF signals excite body tissues, and the received signals are processed through amplifiers, detectors, and digitizers. The computer reconstructs these signals into images, which are finally displayed on film.

4) PET

In vivo cross-sectional images of the physiology, biological function of positron-emitting isotopes, or disease can be obtained using positron emission tomography. This technique uses a radioactive isotope that decays into positrons or positive electrons to identify a chemical molecule with the target biological activity [19]. Almost immediately, the liberated positron collides with an electron, destroying both and releasing two gamma rays in the process. As the two gamma ray photons travel through the surrounding tissue in roughly opposite directions, they are picked up by a circular network of detectors outside the patient.

a) Working of PET

In this technique, the first Radiotracer is injected into the patient body. Many radiotracers are available but FDG (18F combined with deoxy glucose) is considered in most studies. Each tracer is a Positron emitter due to radioactive decay. The emitted positron moves about one millimetre through the body tissue until interacting with an electron, and the two are mutually annihilated, releasing two gamma rays. As they pass through the surrounding tissue, the two gamma-ray photons move in nearly opposite directions, a circular array of detectors records them. A computer rapidly uses a mathematical method to reconstruct the subject's radioactive distribution on a chosen plane, and the resulting image is shown on the screen. This means that PET may evaluate several metabolic processes crucial to the organ's function in a non-invasive regional fashion.

With PET imagery seem significantly coarser and/or blurrier than CT and MR images because of the comparatively small amount of photons that may be captured during an imaging investigation. It produces a 2 or 3D image of the functional processes of the body.

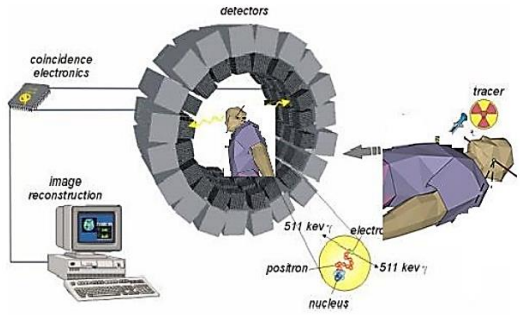

Fig. 8. PET Scanner Working

Figure 8 illustrates the working of A Positron Emission Tomography (PET) scan involves giving the patient a radioactive tracer. When electrons and positron emissions from the tracer combine, two gamma rays (511 keV) are produced that travel in the inverse way. These signals are picked up by detectors that are placed around the patient, and coincidence electronics process them. A computer then reconstructs the data into detailed images for medical analysis.

b) Diagnostic

PET scans are commonly used to identify cancer, heart issues, brain diseases, and central nervous system issues.

III. Attenuation Correction

Attenuation correction (AC) in nuclear medicine imaging, particularly PET and SPECT, addresses the reduction in photon signal due to scattering or absorption as photons pass through different body tissues before reaching the detector, which otherwise leads to reduced image contrast, false defects, and inaccurate quantification of tracer uptake. Early approaches relied on mathematical modelling using emission data or transmission scans with external sources, but these methods were limited by noise and instability. Modern AC techniques, especially CT-based methods, have become standard by providing accurate attenuation maps, while MRI-based methods are used in hybrid systems. Recently, AI-driven approaches, such as DL based synthetic CT generation, have shown promise in improving accuracy and

reducing radiation exposure [20]. Overall, attenuation correction is essential for producing reliable, images of superior quality that facilitate precise diagnosis and efficient treatment planning. Accurately determining the two photons released into space-time by a positron-emitting radionuclide's disintegration is a prerequisite for any observation of a genuine coincidence. The amount of light that reaches the retina depends on mostly absorbed by the body, but the size of the item in the field of view. Attenuation is the term used to describe this lack of detection of genuine coincidence occurrences. Unless adjusted during image reconstruction, it causes significant artefacts in PET images since it is lower on the exterior of the body as opposed to the inside, in the lungs, and particularly in solid tissues, such as bones.

A. CT-based Attenuation Correction

The attenuation of PET image data obtained with PET-CT scanners is adjusted using CT (computed tomography) data. Image artefacts and quantitative mistakes may result from patient movement and the residual CT contrast material, despite the typically accurate nature of CT-based attenuation correction [21]. The difference between the attenuation during a Respiratory movement is the source of the attenuation map based on CT and PET scans, which might introduce bias.

B. MR-based Attenuation Correction

- PET-MR scanners employ MR data to attenuate PET image data; Attenuation correction cannot be performed directly on MR data; instead, the attenuation map must be computed using known attenuation coefficients of various tissue types [22]. The necessary techniques have many caveats, yet dependable PET images may be produced with standardization and careful processing.
- It may be necessary to put the arms up when imaging the pelvic area in order to avoid inaccuracies caused by arm truncation in MRI when the bladder is very active. An excess of iron in the liver might cause underestimated attenuation and poor MRI intensity.
- Dynamic attenuation correction may be included in MR-based motion correction in cardiac PET/MR, which lowers the possibility of attenuation correction artefacts in areas along the lung-soft tissue border.

C. Transmission Scan

Traditionally, while the patient is placed within the scanner, but before the injection of the radiotracer, a second transmission scan is obtained in order to assess the attenuation. An external radioactive positron-emitting source (often 68Ge/68Ga) is used to accomplish the transmission scan. Earlier, generally every morning, a blank scan was conducted using the same source but without the patient. Attenuation correction factors are computed using the transmission and blank scan (≥1.0).

Why AC?

The use of PET and SPECT imaging is expanding beyond its traditional applications in cancer staging and diagnosis to include quantitative indicators for therapy evaluation response or developing personalized treatment plans [23]. However, before the measured signal may reveal information about the response to therapy, a number of adjustments must be made. Physical impacts include photon attenuation and distributed and random coincidences (PET), Tracer uptake levels in the image can be impacted by variations in detector performance, SPECT, the collimator effect, and depth-dependent blur, which are all aspects of geometry-dependent signal response. The primary consequence of photon attenuation in PET imaging.

In SPECT imaging, attenuation is an additional important consideration. After passing through the body, the emission photons from SPECT and PET tracers undergo linear attenuation due to both absorption and scattering. When photons deviate from a straight line due to physical contact, this is known as linear attenuation. Other attenuation channels from the tracer source to the detector understate the uptake activity and cause an inhomogeneous skew of the activity's distribution. Typical artefacts in uncorrected images include negative tracer concentrations in mediastinal areas or increased activity in cutaneous and pulmonary regions (often known as "hot" lungs) (Figure 9).

The absence of air conditioning can also conceal the existence of cold spots or hot characteristics, such solid lesions with somewhat increased tracer absorption, such those that show moderate ischemia on heart perfusion tests [24]. Further information can still be obtained by reconstructing radionuclide images without AC, although. For instance, it can be used to either check for issues with the attenuation map alone

or to check for artefacts caused either mechanically misaligning the emission and attenuation maps or patient movements (Figure 10). Thus, best practices necessitate that images created with and without AC be reviewed for numerous applications.

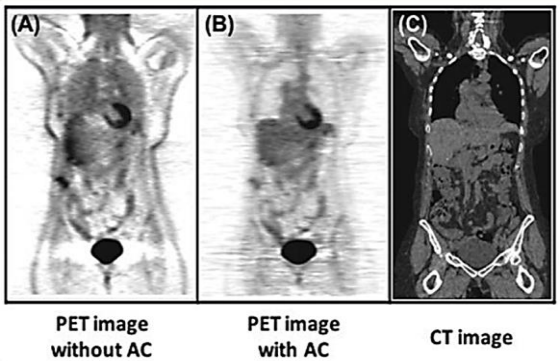

Fig. 9. Photon Attenuation Must Be Corrected for Accurate PET Imaging. A) PET Image Displaying Several Artefacts Without Attenuation Correction; B) CT Attenuation Correction in A PET Image; C) Corresponding CT Image.

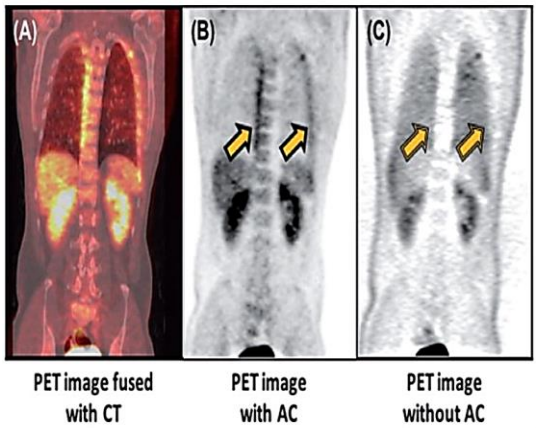

Fig. 10. Artifacts when a Patient Shifted Between CT and PET Scans. A) In the PET/CT Fused Picture, Elevated Tracer Uptake is shown at one Side of the Lung Borders; B) Increased Uptake Value At Lung Borders in a PET Picture with CT-Based Attenuation Correction (arrows); C) Elevated Uptake is not Seen at the Same Sites (arrows) in the PET Picture without Attenuation Correction.

IV. Early Developments in Attenuation Correction

The concept of attenuation correction (AC) in nuclear medicine imaging was developed as a result of a fundamental flaw in both PET and SPECT: photons' interaction with human tissues, which results in their absorption or dispersion prior to their arrival reaching the detector. In the earliest days of clinical PET and SPECT, attenuation was recognized as a major source of image distortion, causing reduced contrast, false perfusion defects, and inaccuracies in quantitative tracer uptake. To address this, researchers began developing mathematical and experimental approaches to estimate and correct for tissue-dependent photon loss.

A. Emission Data–Based Correction

One of the earliest strategies was the use of emission data itself for estimating attenuation maps (μ-maps). This approach, known as "emission-based attenuation correction," attempted to derive both activity distribution and attenuation coefficients from the same dataset. While conceptually appealing, the problem's poorly presented nature made it computationally unstable, requiring heavy assumptions and often producing noisy or biased reconstructions.

B. Transmission Measurements

The measurement of photon attenuation using external transmission sources was another significant advancement. In PET, rotating rod or ring sources of positron-emitting radionuclides such as ^68Ge/^68Ga were commonly used, while SPECT employed sealed gamma-emitting line or flood sources [25]. These transmission scans provided direct measurements of tissue attenuation, enabling the creation of voxel-based attenuation maps. However, drawbacks such as long acquisition times, high noise levels, and misregistration with emission scans limited their clinical applicability.

C. Analytic and Iterative Algorithms

During the 1980s and 1990s, attention shifted toward algorithmic solutions. Early analytic methods, including modified forms of filtered back projection (FBP), attempted to incorporate uniform or non-uniform attenuation models. In SPECT, the Chang method became a landmark development, applying a post-reconstruction uniform attenuation correction factor, which although simplistic, significantly improved diagnostic confidence in myocardial perfusion imaging. Iterative reconstruction algorithms further advanced this field by enabling the incorporation of non-uniform attenuation information directly into the reconstruction process, making corrections more robust and clinically practical.

D. Transition to Hybrid Imaging

By the late 1990s, both PET and SPECT communities recognized the need for more accurate attenuation maps. A ground-breaking answer was

offered by the development of hybrid PET/CT and SPECT/CT scanners, which directly integrated emission pictures with anatomical CT data [26]. CT-based μ-maps offered unprecedented accuracy, faster acquisition times, and reduced noise compared with radionuclide transmission scans, setting a new clinical standard and rendering many earlier approaches obsolete.

E. Historical Significance

The early developments in attenuation correction laid the foundation for the techniques in use today. While emission-based and transmission-based strategies demonstrated the feasibility of AC, the combination of algorithmic innovations and hybrid imaging technologies propelled the field into modern practice. Importantly, this formative period highlighted the shared challenges and common solutions in PET and SPECT, before their trajectories diverged due to modality-specific technological advances. The main attenuation correction methods for PET and SPECT are summarized in Table I.

TABLE I. OVERVIEW OF KEY ATTENUATION CORRECTION TECHNIQUES IN PET AND SPECT

Approach	Key Concept	Strengths	Drawbacks	Typical Era
Emission-Driven AC	Estimates tissue attenuation and tracer distribution concurrently using just emission data (μ-maps).	Eliminates need for extra scans; conceptually straightforward.	Mathematically ill-posed; results prone to noise and instability.	Pre-1990s, primarily experimental.
Transmission Scan–Based AC	Employs external radioactive sources (^68Ge/^68Ga for PET; sealed gamma sources for SPECT) to measure tissue attenuation directly.	Provides a direct measurement of tissue properties; improved quantitative accuracy.	Long acquisition times; potential misalignment with emission data; limited routine clinical use.	1980s–1990s.
Chang Method (Uniform AC)	Applies a uniform attenuation factor post-reconstruction, commonly used in SPECT myocardial studies.	Simple to implement; enhances myocardial perfusion imaging.	Oversimplifies attenuation; fails in anatomically complex regions.	1980s–1990s.
Analytic (Modified FBP) Methods	Modifies traditional filtered back-projection to incorporate attenuation models.	Faster than early iterative techniques; mathematically elegant.	Limited to simple geometries; less accurate in complex cases.	1980s–1990s.
Iterative Reconstruction with AC	Incorporates non-uniform attenuation correction directly into iterative algorithms like MLEM or OSEM.	Highly accurate; adaptable to complex anatomy; practical for clinical use.	Initially computationally intensive.	Emerged in 1990s; became widespread after 2000.
Hybrid PET/CT & SPECT/CT	Combines CT-derived μ-maps with emission scans for direct attenuation correction.	Fast, low-noise, and highly accurate; considered the clinical gold standard.	Adds radiation exposure; dependent on integrated CT hardware.	Late 1990s onward.

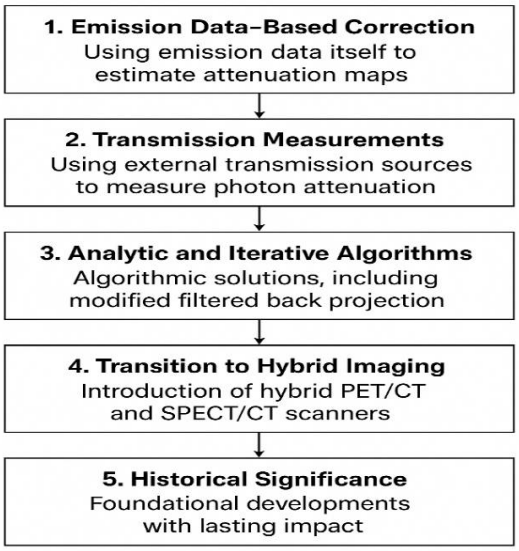

Fig. 11. Stages in Attenuation Correlation

The evolution of attenuation correction (AC) in nuclear medicine imaging. Initially, emission data-based correction used the acquired emission data itself to estimate attenuation maps, though it was limited by noise and instability. This was followed by transmission measurements, where external radioactive sources quantified photon attenuation more directly. Advances in computational methods led to analytic and iterative algorithms, including modified filtered back-projection, improving accuracy and image quality. The shift to hybrid imaging, which combines functional and anatomical data using SPECT/CT and PET/CT scanners, enhancing both quantification and diagnostic utility. Collectively, these developments represent foundational milestones with a lasting impact on modern nuclear medicine imaging (Figure 11).

V. Fundamentals of Attenuation in Nuclear Medicine

The process by which gamma photons lose intensity as they travel through the body and ultimately arrive at the detector is known as attenuation in nuclear medicine. This phenomenon results from interactions between photons and matter, mainly through Compton scattering and photoelectric absorption, which are influenced by photon energy as well as tissue density and composition. Attenuation affects both SPECT and PET imaging, causing photon loss or misdirection, This, if left untreated, can cause artefacts and deteriorate image quality.

The extent of photon attenuation is quantified using the probability of photon interaction for every unit of tissue length is shown by the linear attenuation coefficient (μ) [27]. Different tissues exhibit varying μ-values bones have high attenuation due to their density and atomic composition, soft tissues have moderate attenuation, and lungs have low attenuation due to air content. Understanding these variations is essential for accurately modelling photon behaviour and implementing attenuation correction.

A. Physics of Photon Attenuation

In nuclear medicine imaging, gamma photons emitted from radiotracers traverse various tissues before reaching the detector. During this journey, photons may lose energy or be completely absorbed, a process collectively termed attenuation. Photoelectric absorption and Compton scattering are the primary causes of attenuation, which are controlled by the composition of atoms, tissue density, and photon energy. Knowing the principles of attenuation physics is crucial because it directly affects the accuracy of reconstructed images in both SPECT and PET imaging.

B. Interaction of Photons with Tissues (Absorption, Scattering)

Photons interact with body tissues through two main mechanisms. When a photon imparts all of its energy to an atom, absorption takes place, effectively removing it from the imaging signal. Scattering, particularly Compton scattering, changes the photon's direction and energy, causing it to deviate from its original path. In SPECT and PET, scattered photons reaching the detector can produce misleading signals, creating artifacts or blurring the image. Different tissues, such as bone, soft tissue, and lungs, exhibit varying probabilities of absorption and scattering, influencing regional image intensity.

C. Attenuation Coefficients and Their Significance

A material's likelihood of photon attenuation per unit channel length is measured by the coefficient of linear attenuation (μ). It is dependent on tissue composition and photon energy. Higher μ-values, such as those in bone, result in more significant attenuation, whereas soft tissues and lungs have lower μ-values. Accurate knowledge of μ-values is essential for attenuation correction, enabling reconstruction methods to recover the actual tracer distribution and make up for photon loss.

D. Impact of Attenuation on Image Quality and Quantification

Attenuation, if uncorrected, leads to image artifacts, reduced contrast, and inaccurate quantification of tracer

uptake. In cardiac SPECT, for example, the diaphragm can create apparent perfusion defects, while in brain PET, attenuation from skull bones may distort regional activity measurements. Correcting for attenuation improves image fidelity, enhances diagnostic accuracy, and enables quantitative assessment of tracer distribution, Important for tracking disease development and treatment success.

E. Sources of Attenuation/Scatter Information

To get attenuation Image, there are three standard sources. The first technique involves obtaining an attenuation image by means of a gearbox scan with an emission source [28]. This method can yield precise attenuation values (with the same energy), but it requires more time to scan (2 to 20 minutes) and has poor spatial resolution and significant noise. The second approach uses emission data as the only variable to estimate activity and attenuation. This method is computationally expensive, noisy, and has poor spatial resolution, yet it allows for precise attenuation value calculation without the need for further scans. The third technique involves converting a high-spatial-resolution, low-noise CT image into an attenuation μ-map. Previous studies have looked at creating attenuation images for emission tomography using separately acquired CT data. As PET-CT and SPECT-CT evolved to enable the capture of a well-aligned attenuation picture from a CT scan, the usage of CT-based attenuation correction for PET or SPECT has increased in clinics. By using attenuation data from an extra CT scan that only takes a few seconds, the image quality was greatly enhanced by PET-CT and SPECT-CT.

For scatter corrections, certain SPECT scenarios with energy resolution can be obtained with techniques like the triple energy window (TEW) methodology without the need for explicitly stated or implicitly determined anatomical data. To properly estimate scatter information and an estimated activity image, however, anatomical information is frequently crucial. Numerous techniques for scatter estimation, including MC-based scatter estimation, model-based scatter approximation, convolution-subtraction scatter estimation, and single scatter simulation (SSS), make use of both anatomical and activity images.

F. Examples of Attenuation/Scatter Correction

Figure 12 uses a SPECT-CT example to illustrate the significance of attenuation/scatter correction for non-Patients receiving I-131 radioimmunotherapy for Hodgkin lymphoma. Both the technique used to obtain the original data and the procedure used to conduct this retrospective analysis were approved by the institutional review board [27]. For precise quantitative emission tomography, as shown in Figure 12, attenuation and scatter data must be integrated. A total of 60 images, 128 x 128 bins (4.8 × 4.8 mm), and a 20-minute acquisition time were utilized to generate the first SPECT data. To create a μ-map for attenuation correction, Figure 12 shows the conversion of a low-dose CT image with 128 × 128 × 81 voxels (4.8 × 4.8 × 4.8 mm) using bilinear fitting. To determine the dispersion, TEW was employed. Each SPECT image was rebuilt using the ML-OS-EM technique, which included six subsets and 35 iterations. The reconstruction algorithm's system matrix included the collimator detector response.

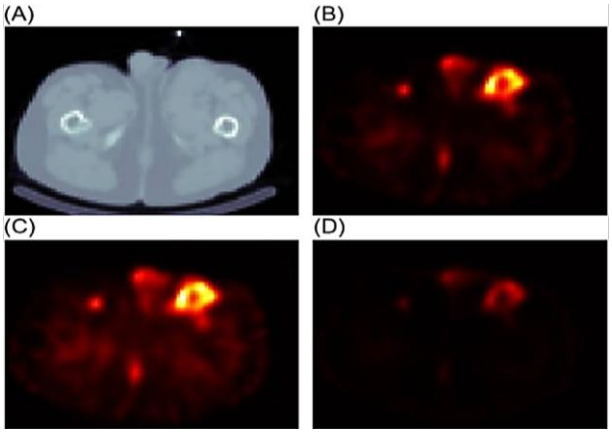

Fig. 12. SPECT Image of a Patient with Both Attenuation and Scatter Corrections

Figure 12 highlights the need to combine scatter and attenuation data for precise quantitative emission tomography. It presents an estimated SPECT image that has been rebuilt using Attenuation correction but no dispersion correction in the ML-OS-EM approach.

VI. WHY HYBRID IMAGING?

It is challenging to get vital functional insights into using conventional clinical methods to measure physiological factors such as receptor density, tissue metabolism, and perfusion, but PET and SPECT imaging offer these insights. Despite these advantages, both modalities lack sufficient morphological data for precise disease localization [23]. Some hybrids are PET/MR, SPECT/CT, and PET/CT devices that combine functional and anatomical modalities to deliver both structural and Session-specific functional data (Figure 13). This synergistic combination not only reduces misalignment errors compared with separately

acquired scans but also makes it unnecessary to do extra transmission scans for attenuation correction (AC), thereby saving time and cost. Furthermore, anatomical imaging contributes essential information for AC, enabling accurate quantification of tracer uptake.

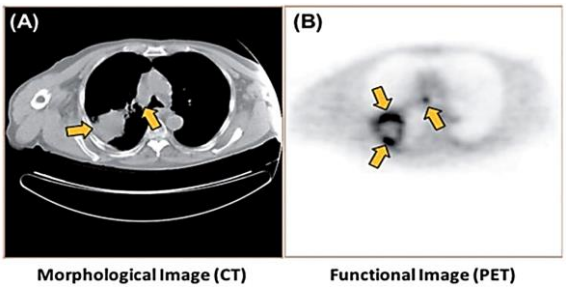

Fig. 13. Hybrid PET/CT Combines Complementary Data: (a) CT Provides Detailed Anatomy without Function, (b) PET Displays Tracer Uptake, but it Lacks Structural Information.

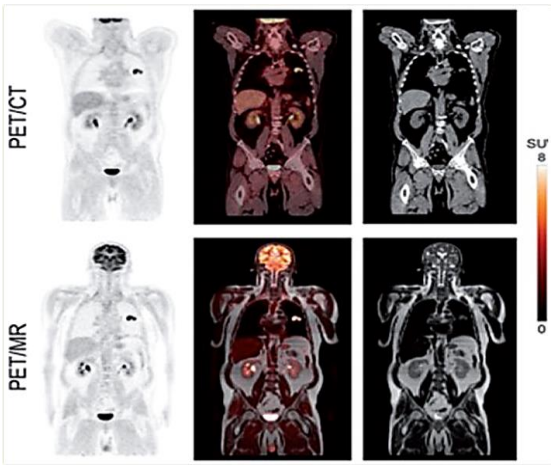

Fig. 14. PET/MR and PET/CT Pictures of the Same Patient [25]. About one Hour After Injecting 15 mCi of 18F-FDG, PET/CT Imaging was Performed, and one Hour and Ten Minutes Later, PET/MR Imaging was Performed.

A comparison of PET/MR and whole-body PET/CT imaging is presented in Figure 14. PET and CT are displayed on the top row as PET-only, fused PET/CT, and CT alone; the bottom row shows PET/MR similarly. A color scale (SUV 0–8) highlights metabolically active regions like the brain and kidneys. The fusion with CT or MR enhances anatomical detail, improving localization and assessment of metabolic activity.

VII. PET/SPECT

Positron emission tomography makes it possible to determine the position and concentration of a material that emits positrons in a cross-section defined by tomography. A positron that has been released interacts with an electron when it is brought to rest, emitting two photons with a combined energy of 511 keV after destroying their masses.= These two photons, which are released at a distance of almost 180 degrees from one another, are known as annihilation gamma-ray photons (Figure 15) [29].

A special method of detecting positrons is based on the annihilation of a positron results in the production of two gamma-ray photons that move in opposing directions.

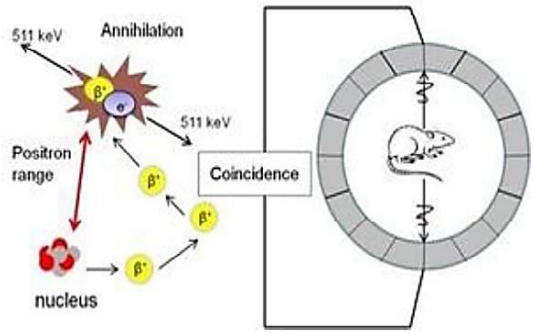

Fig. 15. Schematic Configuration for Positron Emission Tomography.

The discovery of a positron-producing nucleus is made possible when two gamma-ray photons are caught simultaneously by two physically separated detectors along a line. For the sake of this discussion, "coincidence detection" is the circuits' "coincidence resolving time" that establishes if the two photons have arrived at the same time. The usual range for this duration is 10–25 ns, which is long enough to negate the significance of path difference considerations. Therefore, it is believed that the two annihilation photons are coincidental if they reach the two detectors within this time span.

A. Attenuation Compensation in PET

Positron Emission Tomography (PET) has two major advantages over SPECT: fundamental attenuation correction and integrated electronic collimation. The simultaneous detection of two photons with virtually opposite orientations and 511 keV velocities, occurs at a PET source point during a positron annihilation; detectors D1 and D2 capture these photons. In the end, the exponential attenuation factor summed throughout the photon routes determines the likelihood of detection along the line of response. This factor is not dependent on the precise

location of the annihilation site, but simply on the entire path length between the detectors. This property makes attenuation correction straightforward, as a transmission scan can directly measure total attenuation along each line of response, allowing emission data to be corrected by division with the corresponding transmission factor. Additionally, PET inherently achieves electronic collimation, since only coincident detections along a defined line are recorded, effectively rejecting events not aligned with the detector pair and thereby eliminating the need for physical collimators used in SPECT.

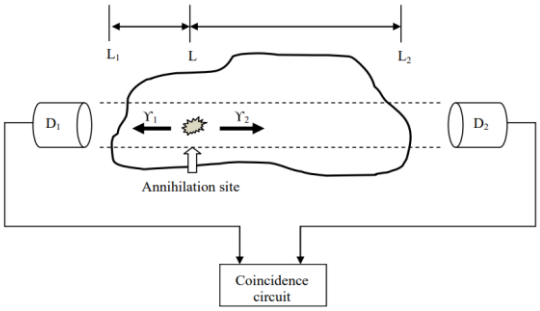

Fig. 16. Schematic Arrangement for Coincidence Detection in PET.

The attenuation factor is constant along the line between the two detectors in Figure 16, regardless of where the positron annihilation occurs, it is one of PET's major benefits. Next, the attenuation factor is identical to the attenuation that a monoenergetic photon beam passing through the item at 511 keV over the length L1L2 would suffer. Consequently, attenuation may be simply accounted for by initiating a transmission study to record the total loss of transmission for every single prediction (data from projections can be used directly without reconstruction).

B. Single Photon Emission Computed Tomography (SPECT)

A nuclear imaging method called SPECT is used to characterize the distribution and degree of activity of gamma-emitting radioisotopes within an item. Gamma rays released by a radionuclide are measured position-sensitively using SPECT (Figure 17). The distribution of radionuclides within the item has a direct correlation with the observed radiation intensity. A collimated detector is used to translate, elevate, and rotate the object in all directions at once to divide the acquisition into horizontal, vertical, and angular sections (Figure 18). The information about each voxel of the examined volume is then obtained by reconstructing the data using analytical or iterative methods.

In tomographic imaging, the three-dimensional activity distributions are ascertained by acquiring the planar images from many angles. On the other hand, SPECT isn't usually thought of as a 3-dimensional imaging problem. However, what is really replicated are two-dimensional slices of the distribution of activity.

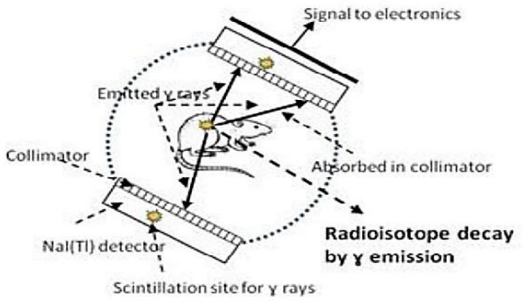

Fig. 17. Schematic Configuration for SPECT

A molecular imaging method that is crucial to medical imaging, SPECT looks at the body in three dimensions (3D) to reveal its functions rather than its anatomy. Producing high-contrast images of tiny organs, tissues, or molecules with only a few of radiopharmaceuticals allows SPECT to measure the kinetic processes involved in the drug-molecule interaction.

C. Attenuation Compensation in SPECT

The attenuation that photons experience on their way from the nucleus that produces them to the detector. The detector is one of the primary obstacles in tomographic imaging of a source that emits gamma rays. The photon energy and the absorber's characteristics both affect how much attenuation occurs. Examine Figure 18's points A and B, which represent two gamma sources of equal power. Attenuation causes the detector to pick up a higher signal from source A compared to source B.

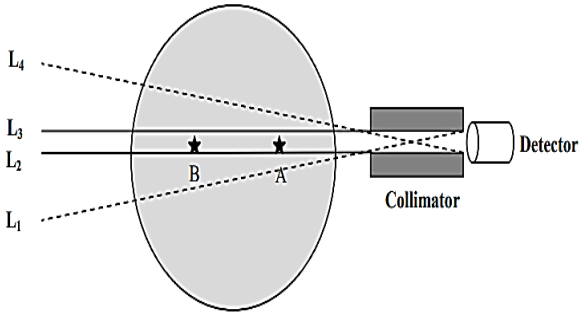

Fig. 18. Formation of Image in SPECT using Collimated Detector

It is possible to describe photon attenuation inside an object as uniform in the most basic case of image reconstruction. Under this assumption, the attenuation of photons emitted from a source point (e.g., point A) follows an exponential decay function, where from the point of origin to the boundary of the item, the exponent grows in direct proportion to the line's length towards the detector while ignoring air losses. In practical applications, however, this problem becomes considerably more complex due to the unknown location of the source and the generally non-uniform distribution of the object's attenuation coefficients. A common approach to address this challenge is to discretize the object into a grid, wherein both the radionuclide concentration and the attenuation coefficient are assumed constant within each grid element. The length of the projection ray within each grid element is then used to calculate the overall attenuation for that particular beam, multiplying it by the corresponding attenuation coefficient, and summing over all grid elements intersected by the ray. To estimate the source activity within each grid element, the projection data produced in this way may be written as a set of solvable simultaneous equations. The accuracy and efficiency of this reconstruction process, however, are strongly dependent on the precision of the assumed attenuation coefficients across the discretized grid.

VIII. Artificial Intelligence in SPECT and SPECT/CT Imaging

The application of AI in nuclear medicine and other medical specialties has effectively transitioned from theory to reality in recent years, thanks to its enormous advancements. Artificial intelligence (AI) methods have great promise as a new resource for genetic testing made possible by the advent of powerful computers and large digital databases that can store vast amounts of information (big data). Local hospitals are putting these strategies into practice and validating them to make sure they complement best practices that support medical personnel in providing everyday clinical services. Pre-reporting activities, dosimetry, patient setup, quality assurance, and other areas of nuclear medicine have all been impacted by AI and its subset of ML approaches. In medical imaging, ML is also used for image interpretation, image reconstruction, and outcome prediction [30], thereby decreasing the workload of nuclear medicine physicians, patient wait times, administered activities, and total imaging time.

Automating tedious and time-consuming procedures is the main goal of AI-based SPECT and SPECT/CT systems. Certain AI applications, such as polar plots and endocardial boundary tracking software, are often employed as valuable prognostic markers in nuclear cardiology. AI has demonstrated great potential in automating cardiac SPECT scans, which might improve the diagnosis and prognosis of coronary artery problems. Automated lung applications based on 3D ML are another well-known example; these apps aid clinicians in outlining and precisely quantifying lung lesions before surgical intervention.

In comparison to traditional techniques, the advent of DL techniques might lead to improved SPECT image reconstruction methods. Originally created as a DL network to reconstruct SPECT images, SPECTNet demonstrated a reduced sensitivity to noise than OSEM-based techniques, allowing for more precise SPECT image reconstruction [31]. The creation of databases such as REFINE SPECT, which provide extensive imaging databases and clinical components, could be another tactic for SPECT and SPECT/CT methods. These datasets are necessary for the development and validation of DL-based techniques for SPECT imaging.

IX. Clinical Implications of Recent Advances in SPECT and SPECT/CT

The primary goal of any tomographic imaging is to ascertain an object's interior distribution just by using outward measures. The following conditions must be satisfied in order for this to be achieved: (a) a full suite of forecasts is obtained, (b) As the forecasts are being made, the internal distribution remains constant regardless of the time or place,(c) While the projections are being made, the detectors' detection sensitivity remains constant, and (d) The precise location of the centre of rotation is known. (The coordinate that indicates the alignment of the generated projections during reconstruction is called the centre of rotation), its accurate placement ensures that the projections shared in their centre.) If it is possible to obtain measurements that meet these criteria, then the internal distribution can be accurately reconstructed. Using clinical examples conducted at the institution in the fields of cardiology, cancer, musculoskeletal disorders, neurology, and infectious diseases, SPECT and SPECT/CT imaging have various clinical effects, which are demonstrated in the sections that follow.

A. Cardiology

SPECT has long been an unmatched imaging technique in nuclear cardiology. The availability of coupled SPECT/CT scanners, which provide anatomical and functional data, has increased the scope. Attenuation artefacts can be reduced with CT-based attenuation correction, making clinical reporting easier and of higher quality [32]. A woman who has struggled with obesity and dyslipidemia for the past 57 years, and hypertension is assessed for chest discomfort in Figure 19 below. IQ was used to do myocardial perfusion studies under stress and during rest. SPECT to check for inducible ischemia on two different days.

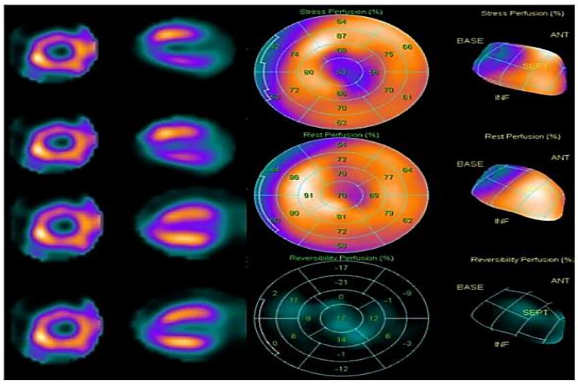

Fig. 19. SPECT Images Show Partial Reversible Apical Perfusion Defects, Confirmed on Polar Maps with the 16-Segment Model.

The myocardium shows hypoperfused areas on the cross-sectional and short-axis images, which may be utilized to identify reversible partial perfusion deficits at the portions that are situated at the structure's extreme top, rear, side, and bottom.

B. Oncology

In nuclear medicine imaging, SPECT/CT has shown to be a potent diagnostic technique for precisely localizing radiotracer distributions, particularly in cancer and thyroid cancer patients [33]. A 71-year-old lady who underwent a full thyroidectomy, Figure 20 shows the results of the neck dissection and the removal of bone metastases from the skull. Metastases to the patient's skull and bones were detected during the course of their follicular thyroid carcinoma. The SPECT/CT images show that the remaining thyroid tissue is localized to the left parietal bone, and the post-therapy scan shows that It is also this bone that contains the remnant cancer at the margins of the operation. Iodine absorption in the neck is also seen by the scan.

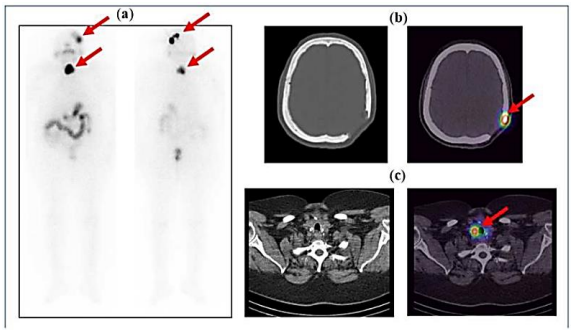

Fig. 20. (a) An Iodine Scan Performed After Treatment Reveals Uptake in the Left Head and Neck, with Physiological Distribution in the Stomach, Colon, Bladder, and Salivary Glands. (b) Tracer Uptake is seen in an Osteolytic Lesion of the Left Parietal Bone on SPECT/CT. (c) Tracer uptake is visible in the Remaining Neck Tissue on Neck SPECT/CT.

C. Musculoskeletal

Nuclear medicine has a long history of using imaging of the musculoskeletal system (MSK), particularly planar whole-body bone scans. Numerous bone illnesses can be diagnosed with it due to its great sensitivity and capacity to show changes in bone before other imaging modalities [34]. Figure 21 shows a case study of a 41-year-old woman who had follow-up for left breast cancer. The scan was carried out following a left-sided MRM procedure and tamoxifen medication. To determine the source of A bone scan was conducted in response to the patient's anterior chest symptoms. On whole-body planar imaging, bone scans show aberrant osteoblastic activity in the sternum; when paired with SPECT/CT images, they pinpoint an osteolytic lesion, leading to a possible diagnosis of bone metastases.

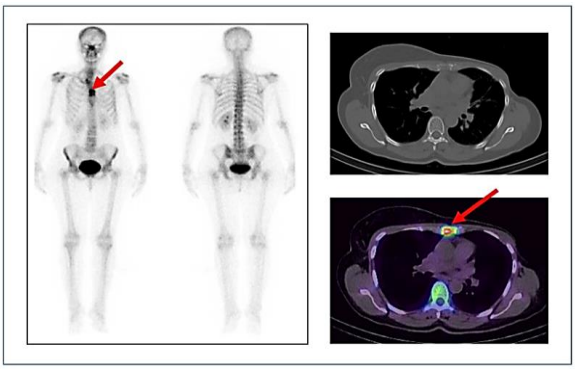

Fig. 21. Whole-Body Bone Scan shows Abnormal Uptake in the Sternum. CT and Fused SPECT/CT Confirm Tracer Uptake at the Osteolytic Lesion Site.

D. Neurology

Nuclear medicine imaging hybrids using SPECT and CT have revolutionized the detection, evaluation, and diagnosis of neurological diseases. This has enhanced lesion identification and localization, which has a favourable effect on patient care [35]. Figure 22 is a clinical case of a child aged 11 who experienced rhinorrhea for a duration of three months subsequent to a head injury. Nuclear medicine specialists ordered him for radionuclide cisternography to check for CSF leaking after his clinical examination and X-rays of the head came out normal. Static and SPECT/CT images were obtained after 125 MBq of Tc99m-DTPA was administered aseptically via intrathecal route. A CSF leak was detected by SPECT/CT, which correctly identified the right ethmoid bone as the location. During surgery, these results were verified.

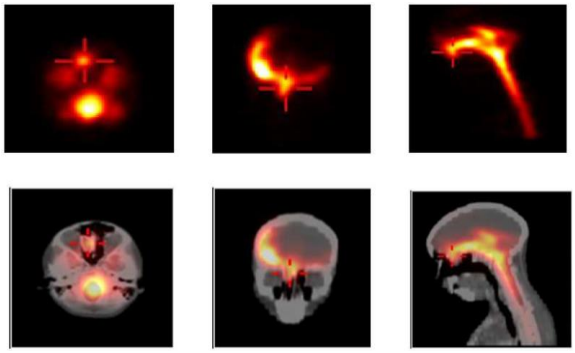

Fig. 22. Planar Images Show Focal Uptake in the Frontal Skull, Localized by SPECT/CT to the Right Ethmoid Bone.

E. Infection

Diagnosing an infection can be extremely difficult for professionals. The capacity to detect and precisely localize the infection focus has been enhanced by Contemporary hybrid SPECT/CT systems with exceptional sensitivity [36]. This is particularly crucial when evaluating diabetic foot in patients with suspected bone or soft tissue infections, fever of unclear cause, and vascular graft infections. A 33-year-old man with an unexplained fever is depicted in Figure 23; all prior tests had been unable to identify the infection's cause. As shown by the arrows, SPECT/CT and Tc-99m WBC whole-body scans identified and located an intra-abdominal abscess, respectively.

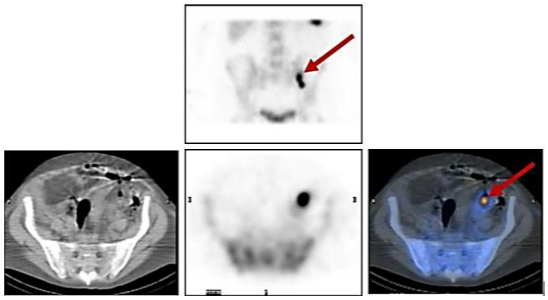

Fig. 23. Planar and SPECT/CT Images Localize Abnormal Uptake to an Intra-Abdominal Peritoneal Abscess.

X. Radionuclide Imaging Technology: PET and SPECT Imaging

The diagnosis and prognosis of several diseases have been greatly impacted during the past 20 years by molecular imaging technologies such as SPECT and PET. The non-invasive feature of these molecular imaging techniques has largely benefited drug discovery and development procedures [37]. These techniques are employed to determine dose schedules, treatment plans, and an understanding of how drugs work. The inception time of SPECT and PET can be dated back in the 1950s and 1960s. PET imaging was the first of the mainstay modalities to be demonstrated, previously hypothesized in 1950 by Brownell and Sweet. Kuhl and Edwards developed SPECT brain imaging, which they formerly described in 1963 and optimized over multiple restatements, culminating the Mark IV system in 1976.

In these techniques, a radionuclide is synthetically introduced into a biomolecule (a ligand/peptide/antibody/antibody fragment) of possible biological significance and administered to a subject (animal or patient). After the radiotracer is administered to a subject, the consequent uptake of the radiotracer is quantified over time and used to attain evidence about the physiological, cellular, and molecular processes of interest.

A. Radioactive Decay and Types

Radioactivity is the outcome of nuclear instability and the spontaneous decay of unstable atomic nuclei. Decomposition can emit a variety of intense ionizing radiations, including particles and electromagnetic radiation. Chemical compounds known as "radiotracers" have one or more atoms swapped out for radioisotopes.

The physicist Ernest Rutherford and his associates discovered that the decay of radioactive substances

releases three distinct categories of radiation six years after Henri Becquerel of France discovered radioactivity in 1896. According to their penetrating power, these radiations were dubbed alpha, beta, and gamma rays (Figure 24). They were identified as high-energy photons, electrons, and helium nuclei, respectively. The word "isotopes" was first used by Soddy in 1913 to refer to atoms of an element that have the same chemical characteristics but differ in atomic weight. Radioactivity is defined as the transformation of one chemical element into another by γ radiation or the release of α or β particles, according to a nuclear disintegration hypothesis (Figure 24).

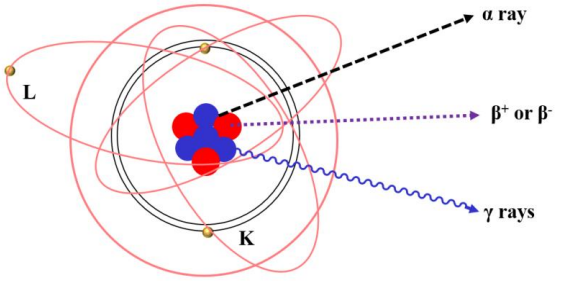

Fig. 24. Radioactive Decay Showing α, β and γ Emission

Various types of Radioactive Decay Radioactive decay can be categorized into two main divisions: a) First, which includes a change in the mass number (A) of a radionuclide, and b) Second, where each Isobaric decay occurs when the mass numbers of the father and daughter radionuclides are equal. In Table II, four primary categories are addressed.

Alpha Decay- Nuclear decay causes an unstable nucleus to change into a different element, creating a particle with two protons and two neutrons. In high atomic number elements like 238U, 230Th, and 226Ra, alpha decay is typically seen. These radionuclides may potentially release γ photons in addition to α particles. Because A>210 radionuclides are big, they need to emit α particles to becoming smaller and more stable. It shows in Equation (1):

$$^{226}_{88}Ra \rightarrow ^{222}_{86}\mathrm{Rn} + ^{4}_{2} \propto \quad (1)$$

Beta decay: The beta decay process begins when an atom's nucleus contains an overabundance of protons or neutrons. Most beta decays fall into one of two categories: The electron and an antineutrino are the products of positive beta decay, whereas the neutrino and positron are the by-products of negative beta decay. On the other hand, positive beta decay happens far less often than negative beta decay.

Positron decay: Radionuclides which lack neutrons are generally unstable and decay to release positive charges either through positron emission or electron capture. These other techniques, known as inverse beta decay, are used to reach the ground state when an unstable nucleus lacks neutrons [38]. Lower atomic-numbered elements are more susceptible to positron emission. Positron emission proceeds with the generation of a daughter nucleus having atomic number (Z−1), leaving the mass number unaffected. Positron emission is responsible for annihilation events.

XI. PET Radionuclides and Their Clinical Applications

In clinical and medical research, the majority of PET radiopharmaceuticals are labelled with the four common PET radionuclides: ^{15}O, ^{13}N, ^{11}C, and ^{18}F. Metal radionuclides, however, are also employed in PET imaging. This section delves into the various radiopharmaceuticals and PET radionuclides and their clinical uses.

A. PET Radiopharmaceuticals in Oncology

[^{18}F] labelled compounds - ^{18}F is one of the most commonly used PET radiopharmaceuticals owing to its stable radio isotopic nature. Fluorine is a highly electronegative atom (4.0) when compared with hydrogen (2.1). Moreover, in vivo, carbon-fluorine (C-F) bonds are more robust and stable than C-H bonds. Thus, replacing hydrogen with fluorine in the biological system potentiates the half-life of the radiopharmaceutical within the organism. This in turn affects Protein-binding kinetics, biodistribution, and molecular metabolism [39]. [^{18}F] fluorodeoxyglucose ([^{18}F] FDG), the most effective PET radiopharmaceuticals are absorbed by cancerous cells with increased glycolytic and metabolic rates.

[^{11}C] labeled compounds - The short half-life of ^{11}C (~20.4 mins) ensures that the radiopharmaceutical does not involve extensive exposure and makes it possible to carry out several investigations quickly. [^{11}C]-choline tracers are used in their ease of absorption by cancer cells during cell proliferation, which leads to the diagnosis of prostate cancer. [^{11}C]-acetate is widely used in Renal cell carcinoma, bladder cancer, and urological cancers. [^{11}C]-erlotinib, a small molecule radiotracer, can use PET scans to identify colorectal and lung cancers.

[^{124}I] - Labeled Compounds- These radiotracer molecules play a dual role in cancer diagnosis, i.e., they serve both as an imaging agent and provide therapeutic benefit. The therapeutic property of ^{124}I radiopharmaceutical is due to the physical characteristics and extended half-life (~4.18 days) of the positron-emitting isotope of iodine. These radionuclides can also be used in mAb development for the potential cure of thyroid and parathyroid cancer [40]. ^{124}I-tagged small molecules are tested for various targets: ^{124}I-dRFIB, ^{124}I-IUdR, and ^{124}ICDK4/6 inhibitors of cell proliferation; ^{124}I-MIBG for adrenergic activity; ^{124}I-hypericin targeting protein kinase C; ^{124}I-IAZA and ^{124}I-IAZG as hypoxia agents; and ^{124}I-FIAU against herpes virus thymidine kinase. Table II lists some important radionuclides and their corresponding radiopharmaceuticals used in cancer diagnosis.

TABLE II. PET RADIOPHARMACEUTICALS USED IN ONCOLOGY

Radiotracer	Disease	Molecular Target	Function	Properties
[methyl-^{11}C] methionine	Urinary, gynaecological, liver, and lung cancer	Two systems, one dependent on sodium and the other on L-type amino acid transporters	Imaging the rate of protein synthesis	The short half-life of [11C] restricts availability for PET scanning; [11C]MET has also been widely used in various brain tumours
[^{11}C]CO	Wide applications in clinical research (amides, ketones, acids, esters, and urea's)	A variety of chemotypes	The production of a wide range of drug-like molecules and radioligands	Requires the presence of transition metals (e.g., Pd) as reagents; poor solubility in organic solvents and high dilution in inert gas
[^{11}C]choline	Prostate cancer	Phospholipid synthesis	Tumour imaging; diagnostic agent	Salt vector; as proliferation of cancer cells increases, tumour cells exhibit increased uptake of the radiotracer
[^{18}F] F-choline	Prostate cancer	Phospholipid synthesis	Primary staging, biochemical recurrence	Salt vector; greater accuracy compared to [18F]FDG
[^{18}F] afatinib	Lung carcinoma, colorectal cancer	Epidermal growth factor receptor	Detection of EGFR-positive tumors	Small molecule
[^{124}I] Icodrituzumab	Hepatocarcinoma	Glypican 3	Detects tumor localization in most patients with HCC	Antibody vector
[^{124}I] Igirentuximab	Renal cell carcinoma	Carbonic anhydrase 9	Discriminates between clear-cell RCC (ccRCC) and non-ccRCC	Antibody vector
[^{64}Cu]-DOTA-AE105	Breast, lung, colorectal, prostate, and bladder cancer	uPAR-PET ligand	Several investigations conducted to validate it in a preclinical setting found it to be predictive of cancer invasion and metastasis.	Peptide antagonists AE105; promising diagnostic/imaging; first in-human use in 2013

[^{68}Ga] citrate	Prosthetic joint/bone infections	N.A.	Diagnosis of bone infection	[68Ga] citrate has additional advantages over [67Ga] for analysis of bone infections
[^{89}Zr] Zr-bevacizumab	Solid malignancies; particularly malignant breast lesions	Vascular endothelial growth factor receptor	Early detection; VEGF-A overexpression	Antibody vectors

B. PET Radiopharmaceuticals in Neurology

PET imaging has helped researchers better understand the pathophysiology of several neurological disorders. Investigations on metabolism, receptor binding, and changes in local blood flow have all been conducted using it. One of its primary functions is to shed light on complex neurological disorders such as Huntington's disease (HD), Parkinson's disease (PD), multiple sclerosis (MS), and Alzheimer's disease (AD), and dementias. Some of the important PET radiopharmaceuticals used in neurodegenerative diseases are enlisted in Table III PET radiotracers can quantify target-ligand interactions in humans with high selectivity, providing information on disease pathology, thanks to the CNS molecular sensitivity. Radiopharmaceuticals with specific applications in brain imaging include [^{18}F]-FDOPA tracers for dopamine synthesis in schizophrenia and Parkinson's disease, [^{18}F]-FDG analogues for detecting changes in glucose metabolism and translocator proteins in Parkinson's and Alzheimer's diseases [41]. Additionally, [^{11}C] -PIB compounds are used to track the accumulation of amyloid β plaque in AD.

The selectivity of a PET tracer is what defines its usefulness and applicability, in spite of the fact that the tracer's BBB-crossing capability is paramount. a molecular weight below 500 kDa, a lipophilic coefficient between 1 and 5, and a topological polar surface area of less than 90 Å2. It is possible to identify abnormal amyloid deposits in brain tissue using certain benzothiazole and benzoxazole derivatives. These include [^{18}F]-flutemetamol, [^{18}F]-florbetapir, and [^{18}F]-florbetaben. [^{18}F]-AV-1451 and [^{18}F]-THK are two tracers that aid in determining the rates at which tau proteins aggregate [42]. Adenosine 2A receptors (A2A) are GPCRS that are heavily targeted in a variety of neurological illnesses and are targeted by CNS neurotransmitters. In this instance, [^{11}C] -TMSX and [11C]-SCH442416 are the most trustworthy tracers created to target A2A. Table III summarizes PET radiotracers, their targets/diseases, imaging functions, and key properties, highlighting their use in brain disorders, tumors, psychiatric conditions, and neuroendocrine tumors.

TABLE III. PET RADIOPHARMACEUTICALS USED IN NEUROLOGY

Radiotracer	Molecular Target / Disease	Function	Properties
[11C] MET	Brain gliomas and metastases	Differentiation of tumor regrowth; delineation of gliomas	Tracer's stability in its final formulation is not well documented in the literature
N-[11C]-methyl-flumazenil	Damage to neurones, epilepsy, penumbral infarction caused by a stroke, and Alzheimer's disease	Locates GABAA receptors by binding to their benzodiazepine sites	Excellent kinetic properties for image quantification
[11C] raclopride	Psychiatric disorders, PD, addiction, ADHD, schizophrenia	Tracer for dopamine function in the striatal cortex	Most widely used PET radiotracer for measuring DA changes at the synaptic level

[11C] UCB-J	Targeting synaptic vesicle proteins SV2A; epilepsy; diseases with synaptic loss	Imaging SV2A expression in synaptic vesicles	Leading SV2A tracer; good selectivity, fast kinetics
[11C]MK-3168	Pain, addiction, Tourette syndrome	Fatty acid amide hydrolase–associated receptors	Slow kinetics and rapid metabolism in humans
[11C]PS13	CNS enzyme dysfunctions	Imaging COX-1	Limited data; low plasma free fraction; suitable kinetic profile
[18F] FET	Brain tumors; gliomas	Does not serve as substrate to protein synthesis; glioma imaging	Highly specific for glioma; unaffected by BBB permeability; overcomes [18F]FDG limitations; evaluation in nonclinical research still lacking
[18F] AV-1451	Tau proteins (tauopathies), AD	AD assessment; distinguishes disease stages	High selectivity over amyloid; fast kinetics
[18F]MK-6240	AD imaging	Imaging neurofibrillary tangles	Low binding in healthy controls; strong correlation with cognitive AD scores
[18F] UCB-H	Targeting synaptic vesicle proteins SV2A	Binds synaptic vesicle glycoprotein 2A	Lower sensitivity vs. [11C]UCB-J
[18F] FIMX	PD, addiction, epilepsy, neuropathic pain, depression	Targeting metabotropic glutamate receptors (mGluR1)	Reaction time in vivo is short and effective.
[18F] BCPP-EF	Targeting mitochondrial complex 1 (MC1)	Quantitative imaging of MC1 activity in brain	Large dynamic range in vitro, appropriate kinetics, and high brain uptake
[64Cu]Cu-SARTATE	Neuroendocrine tumors	Targeting somatostatin receptor 2	Peptide vector

C. PET Radiopharmaceuticals for Cardiovascular Diseases

Nuclear cardiology has extended its spectrum over the past few years and is applied in the detection of heart function, circulation of blood, non-invasive heart inflammation and myocardial viability imaging [43]. [13N]-ammonia is a potential tracer for measuring myocardial blood flow or myocardial uptake. For myocardial perfusion imaging, inorganic radiopharmaceuticals with 13N and 15O labels have been utilized extensively. 18F-fluorodopamine and 11C-epinephrine are examples of small organic tracer molecules that were helpful in imaging the heart's presynaptic sympathetic nervous system. Cationic radiotracer like [^{82}Rb]-chloride targets Na+ /K+ ATPase cotransporters and helps in myocardial perfusion imaging. A wide range of PET radiopharmaceuticals used for cardiovascular disease imaging is given in Table IV:

TABLE IV. PET RADIOPHARMACEUTICALS USED IN CARDIOLOGY

Radiotracer	**Disease**	**Molecular Target**	**Function**	**Properties**
[^{82}Rb] chloride	Cardiac conditions	Cardiac tissue	Diagnostic; monitoring the cardiac flow	Low delivered radiation exposure for a rest/stress test
[^{15O}] H2O	Tumour, cerebral, and myocardial perfusion	N.A.	A device that measures the amount of blood flowing to the brain quantitatively	The short half-life of [15O] results in challenges in clinical use

[^{13}N] NH3	Cardiovascular events, PC, and encephalopathy	Heart, hepatic, renal, and cerebral tissues	Imaging agent for assessing regional blood flow in tissues; for elucidation of NH3 metabolism in patients with hepatic encephalopathy; potentially a tumor imaging agent	[13N]NH3 enters the myocardium through the coronary arteries; well-validated radiotracer for clinical management; also used in PC due to the up-regulation of NH3 during glutamine synthesis in tumors
[^{15}O]CO	Cardiovascular events	Myocardial tissue	Myocardial function	The most widely used tracer for non-invasively determining blood volume and oxygen consumption
[^{18}F] flurpiridaz	Myocardial perfusion	Mitochondrial complex I	Diagnostic/imaging	Novel PET tracer
[^{18}F] macroflor	Atherosclerosis	Macrophage-targeted polyglucose nanoparticle	Immunoimaging; nanoparticle uptake	Risk assessment for atherosclerosis using noninvasive immune system testing
[^{64}Cu] DOTAECL1i	Lung inflammation	Type 2 chemokine receptor	Detection of CCR2-directed inflammation	Sensitive and specific detection of $CCR2^{+}$ cells

D. PET Radiopharmaceuticals for Bacteria Imaging

The research investigations that dealt with bacterial PET imaging were categorized by Auletta et al. according to the types of bacteria they studied. Gram-positive bacteria imaging produced better imaging results compared to other strains used during the studies [44]. ^{124}I-labeled FIAU revealed better results in animal models than in humans. [^{18}F]-FDG-6-P agents can distinguish between infection and sterile inflammation and are highly expressed in several bacteria. Table V enumerates some PET radiopharmaceuticals used in bacterial imaging.

TABLE V. PET RADIOPHARMACEUTICALS USED IN BACTERIA IMAGING

Radiotracer	Type of Bacteria	Properties
[^{18}F] FHM (maltohexose)	S. aureus	Superior to FDG for distinguishing between infection and non-infection inflammation
[^{18}F] FDS (sorbitol)	K. pneumoniae	Better than FDG for identifying inflammation-based lung infections
[^{18}F] maltotriose	N.A.	Animal bacterial infection imaging: potential clinical uses
[^{18}F] FDS	E. coli, Enterobacteriaceae	Identification and treatment monitoring; infection diagnosis
[^{18}F] FDG-6-P	S. aureus	Ability to distinguish between inflammation and infection
[^{18}F] isonicotinic acid	M. tuberculosis	Localising infectious foci non-invasively; only tried on mice
[^{18}F] FIAU	E. coli, P. aeruginosa	Pathogens that have been engineered to assess experimental treatments

[^{18}F] PABA	S. aureus	Non-invasive method for tracking, identifying, and detecting infections
[^{68}Ga] TAFC / [68Ga]FOXE	A. fumigatus	Very potential for highly sensitive infection detection
[^{64}Cu] ProT (prothrombin)	S. aureus	Non-invasive detection with an analog of ProT
[^{64}Cu] JF5 mAb	A. fumigatus	Localized aspergillus infection
[^{18}F] maltose	E. coli	Identifying drug resistance; promising for bacterial infection imaging
[^{18}F] trimethoprim	E. coli, P. aeruginosa, S. aureus	Infection imaging
[^{68}Ga] UBI-29-41	S. aureus	Non-toxic, identifies infectious foci in humans; correlated with degree of infection; needs further studies
[^{68}Ga] UBI-31-38	S. aureus	Good localization of infection site; promising results in humans
[^{68}Ga] TBIA101 (depsidomycin derivative)	M. tuberculosis, S. aureus	Imaging inflammation but not necessarily infection; non-specific
[^{124}I] FIAU (fialuridine)	S. aureus	Well tolerated but of limited value for detection of prosthetic joint infection; low image quality/specificity
[^{11}C] PABA (para-aminobenzoic acid)	E. coli	Imaging living bacteria in humans

E. PET Radiopharmaceuticals for Inflammation/Infection

Infection or inflammation is directly or indirectly associated with a number of disorders. Thus, molecular imaging of inflammation in a diversity of situations (such as atherosclerosis, autoimmune disorders, stroke, AD, and even cancer) offers a wealth of information about the diagnosis or prognosis of a disease. B cells are one of the main therapeutic targets essential for controlling immunological responses. BTK, a cytoplasmic tyrosine kinase that B cells express, is being researched as a potential therapy for B-cell cancers. BTK inhibitors that are radiolabelled are crucial for the treatment and surveillance of B-cell-mediated illnesses. [^{11}C]- ibrutinib a potential PET imager used for inflammation imaging presented >98% radiochemical purity and 19.89 to 20.15 min half-life.

11C or 18F-labelled is quinoline carboxamide derivatives are used in PET imaging of peripheral tissue translocator proteins, which are expressed during inflammation. PET imaging has shown encouraging outcomes in the identification of atherosclerosis, lung lesion absorption, neuroendocrine tumour imaging, etc. [^{18}F]-FDG is the most effective agent for biopsies since it can pinpoint the sites of infection with the highest activity. It also has a significant effect on imaging for big vessel vasculitis and aids in therapy monitoring and management.

XII. SPECT Principle and Radiopharmaceuticals

A SPECT machine combines the object is followed by a group of one to four gamma cameras that spin around it [45]. Gamma cameras designed specifically for patient rotation and are covered in Table VI can be used to assess the spatial distribution of radionuclides within tissues. Multiple gamma cameras improve spatial resolution and detector efficiency. Then, using the camera-collected projection data, three-dimensional images are created. Figure 25 illustrates the fundamental idea behind SPECT imaging.

TABLE VI. Commonly used radionuclides for SPECT imaging

Nuclide	**Half-life (h)**	**Principal photon emission energies (MeV)**	**Type of emission**
123I	13.2	0.16	Electron capture

99mTc	6	0.14	Isomeric transition
111In	67.9	0.17 / 0.25	Electron capture
67Ga	78.3	0.09 / 0.19 / 0.30	Electron capture
201Tl	73.1	0.17	Electron capture

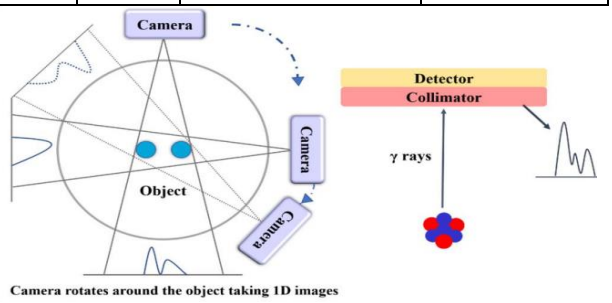

Fig. 25. Principles of SPECT Imaging

A. SPECT Radiopharmaceuticals

SPECT radiopharmaceuticals employ gamma (γ) radiation to diagnose infections, cancer, and neurological illnesses [46]. The advantage of these compounds' extended half-lives is that they allow for lengthier SPECT imaging experiments. Some frequently used technetium (99mTc) labelled SPECT radiopharmaceuticals are displayed in Figure 17. The important features required for a good SPECT radiotracer are:

Easy availability

- Carrier free
- Non-toxic
- Free from the emission of α and β particles (with little emission)
- A biological half-life that does not exceed the duration of the research
- Suitable energy range
- Stable enough to form coordinated covalent connections with the unknown material through chemical reactions.

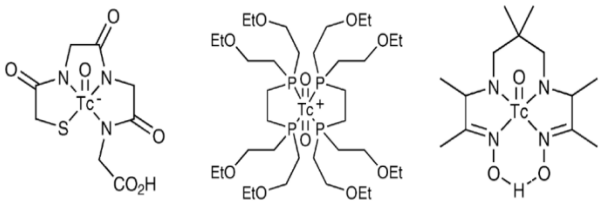

Fig. 26. Examples of 99mTc radiopharmaceuticals

Figure 26 shows three technetium-based coordination complexes with distinct ligand environments. The first structure is a technetium(V) complex coordinated with a dithiol-containing chelator and a carboxylate group, indicating potential use in radiopharmaceutical targeting. The second structure is a technetium(V) oxo complex with a hexakisphosphine ligand, where the technetium is stabilized in a pseudo-octahedral geometry, commonly explored in imaging or catalysis applications. The third structure is a technetium(V) complex with a hydroxamate-type ligand and sterically bulky substituents, suggesting enhanced stability and potential biological compatibility for diagnostic purposes. Together, these structures illustrate the versatility of technetium coordination chemistry for radiopharmaceutical design.

XIII. Application of SPECT Imaging

During SPECT imaging, the clinician must have prior knowledge about: a) the goal of the scan b) the associated risk to the patient, and c) the expense of the isotope. SPECT imaging not only depends on the selection of the correct radioisotope, but the main achievement lies in the fact that the isotope must be effectively attached to a physiologically active ligand that interacts with bodily tissues to transport it to the intended site. There are other factors than choosing the right radioisotope that affect SPECT imaging [47]. The SPECT scan has been very useful in the medical industry, particularly for the detection of malignancies, cardiovascular illnesses, and neurological disorders. Additionally, SPECT scans can detect a wide range of non-neurological and non-cardiac disorders, such as pulmonary embolism, osteomyelitis, spondylolysis, parathyroid failure, and abscess localization.

SPECT imaging in Oncology- SPECT imaging has played a wholesome role in clinical oncology in determining which tumours overexpress certain receptors. Melanomas, gastrin-releasing peptide, integrin αvβ3, somatostatin, breast, brain, small cell lung, and colorectal tumours are all affected by these

receptors. Furthermore, these receptors impact gastrin-releasing peptide, ovarian, pancreatic, small cell lung, and colorectal cancers [48].

SPECT Radiopharmaceuticals for Cardiovascular Events- Tc-labelled radiopharmaceuticals have demonstrated favourable outcomes in coronary artery disease (CAD) diagnosis and risk assessment. There are three SPECT imaging agents that have shown promise; they are [201Tl]-Cl, [^{99m}Tc(I)]-sesamoid, and [^{99m}Tc(V)]-etoformin. The applicability of these diagnostic agents relies based on their favourable pharmacokinetic characteristics (rapid clearance, linear correlation between blood flow and absorption, high first-pass extraction, and half-life).

[^{99m}Tc(V)] is an imaging agent for SPECT that is frequently used to diagnose neurological diseases, including Parkinson's disease, and other similar conditions. -isoflurane and -HMPAO [^{123}I] [^{99m}Tc(I)] Amyloid beta imaging (TRODAT-1) makes use of imidazopyridine molecules based on 123I.

A. Difference between PET and SPECT Imaging

There is extensive use of both SPECT and PET imaging agents in the medical field for the diagnosis of different disease pathologies. However, both have unique features which make them better than each other. Table VII highlights the benefits, drawbacks, and clinical applications of both PET and SPECT imaging agents, highlighting their differences from one another.

TABLE VII. COMPARISON BETWEEN PET AND SPECT IMAGING AGENTS

Method	**Advantages**	**Disadvantages**	**Clinical Use**	**In vivo Animal Use**
PET	- High sensitivity - 3D acquisition - Good resolution within a physical limit	- Isotopes are of short half-life - Isotopes produced in cyclotrons - Expensive process - Higher tissue dose required	- [^{18}F]FDG is a routine imaging agent in the diagnosis of cancer - Special application in neurology and cardiology	Currently evolving: - microPET - High-density avalanche chamber
SPECT	- Resolution limited by technology (submillimeter) - Low sensitivities - Can differentiate between isotopes with different radiation energies	- 2D planar images - Semiquantitative data only	- Readily available tracer - A wide range of clinically tested tracers available	- Pinhole collimator - Dedicated cameras evolving

XIV. LITERATURE REVIEW

This section briefly reviews recent attenuation correction methods and deep learning–based imaging models. Each approach demonstrates improved accuracy and artifact reduction across various SPECT and PET imaging applications discussed in table VIII.

Kawakubo et al. (2024) showed that conventional SPECT voxel values significantly deviated from PET in basal anterior and mid anteroseptal/inferior regions under stress and rest, whereas SPECTSPT showed no significant errors in stress and only minor deviations in resting states. Moreover, conventional SPECT demonstrated significant overscoring in inferior wall regions during stress, while SPECTSPT exhibited no such overscoring, with only moderate variations in segment #4. These findings suggest that the PET-supervised SPECTSPT model effectively corrects inferior wall attenuation, offering a useful and affordable technique to improve cardiac perfusion imaging diagnostic accuracy, especially in standalone SPECT systems [49].

Bouchareb et al. (2024) analyses the clinical applications, prospective directions, and advancements in imaging technologies for SPECT and SPECT/CT. This research primarily focusses on quantitative approaches, image reconstruction techniques, several

related subjects, such as detector materials, camera head and collimator designs, signal amplifier devices, and many more. More efficient energy and spatial resolution detectors are replacing the bulky photomultiplier tubes (PMTs) with alternatives Avalanche photodiodes (APDs) and position-sensitive photomultiplier tubes (PSPMTs) are two examples. Only SPECT cameras are capable of provide a new generation of cutting-edge cardiac imaging. Making use of a CdZnTe semiconductor detector or an L-shaped camera head, the novel design integrates specialist collimators with traditional sodium iodide detectors (NaI(Tl)). Particularly at specialist clinical facilities, the new design's clinical advantages include reduced overall size, better image quality, quicker scanning periods, more patient comfort, and fewer claustrophobic effects. Implementing resolution-recovery iterative reconstructions is also responsible for these observable gains. Many attempts have been made to use camera-specific models to make SPECT and SPECT/CT imaging quantitative tools [50].

Chen and Liu (2023) SPECT and PET findings in AC can be essentially categorized into two categories: indirect and direct techniques. After reviewing the fundamentals and limits of non-DL AC methods, moved on to examine the current state and future prospects of DL-based approaches to SPECT and PET AC. To create CT images or artificial μ-maps, indirect AC methods use neural networks to change transmission, emission, or magnetic resonance data, which aids in AC reconstruction. Direct AC methods eliminate the need to create v-maps or CT images beforehand, and instead use data from PET or non-attenuation-corrected SPECT scans to instantly predict images from AC SPECT scans. When compared to non-DL approaches, the performance of these AC methods based on deep learning is competitive or even superior [51].

Du et al. (2023) study retrospectively evaluated 260 individuals who used two separate scanners to perform 99mTc-TRODAT-1 SPECT/CT scans, comparing Chang-AC with DL-based AC methods, including indirect DL-ACμ (estimating attenuation maps), direct DL-AC (generating AC SPECT images), cross-scanner training (cDL-ACμ and cDL-AC), and ensemble training (eDL-ACμ and eDL-AC). Ordered-subset expectation-maximization with dual-energy scatter correction was used for the reconstructions, and the asymmetry index (%ASI), specific uptake ratio (SUR), This performance was assessed using structural similarity index (SSIM) and normalised mean square error (NMSE). All DL-based AC techniques beat Chang-AC, according to the results, with DL-ACμ having the highest accuracy, followed by DL-AC and ensemble/cross-scanner techniques. For DL-ACμ, SUR and %ASI were closest to CT-AC, and training tailored to a scanner performed better than training across scanners and ensembles. DL-based AC performed better than Chang-AC in respect to practicability, resilience, and efficiency [52].

Mostafapour et al. (2022) evaluated the use of ResNet and U-Net deep convolutional neural networks for direct Myocardial perfusion SPECT (MPI-SPECT) attenuation correction (AC). The input consisted of 99 patients' non-attenuation-corrected SPECT images, with CT-based AC SPECT as reference and Chang's method as comparison. Validation on 19 subjects included voxel-wise errors, Total perfusion deficit (TPD), structural similarity index (SSI) and peak signal-to-noise ratio. DL models showed strong agreement with CT-AC; ResNet and U-Net outperformed Chang's technique (ME: 25.52 ± 33.98, SSI: 0.93 ± 0.09), with MEs of −6.99 ± 16.72 and −4.41 ± 11.8 and SSIs of 0.99 ± 0.04 and 0.98 ± 0.05, respectively. Clinically, TPD values from ResNet (12.78 ± 9.22%) and U-Net (12.57 ± 8.93%) closely matched CT-AC (12.84 ± 8.63%), while Chang's method overestimated (16.68 ± 11.24%). These results highlight the reliability of DL-based AC for MPI-SPECT imaging [53].

Omidvari et al. (2022) studied the lutetium background radiation for attenuation correction in total-body PET by using a 3D whole-body XCAT phantom in the uEXPLORER PET scanner to perform Monte Carlo simulations. The focus was on the recently made possible ultralow-dose PET scans. Compton scattering, shorter scan times, and a larger acceptance angle were all examined in relation to PET quantification. A one-meter-long scanner, a normal twenty-four-centimeter-long scanner, and a twenty-minute full-body scan on the uEXPLORER were used to assess the accuracy of lutetium-based attenuation correction. The mean bias in all the organs that were scanned for 20 minutes in a whole-body scan was within ±10% of ground-truth activity maps, and Quantification and lesion contrast were very little impacted by any of the large axial field-of-view scanners. Reducing the scan length to 5 minutes or using a decreased acceptance angle of 17° had an impact on quantification in several organs [54].

Yang et al. (2021) study of 100 patients undergoing 99mTc-tetrofosmin cardiac SPECT/CT at Yale New Haven Hospital, they created a direct AC approach based on DL to produce attenuation-corrected SPECT (SPECTDL) straight from noncorrected infrared (SPECTNC). A convolutional neural network was trained and evaluated against CT-based AC (SPECTCTAC) using voxelwise and segment wise analyses with the 17-segment American Heart Association model. Compared with SPECTNC, which showed larger variability and segmental errors ranging from −35% to 21%, SPECTDL achieved stronger voxelwise correlation with SPECTCTAC (97.7% ± 1.8% vs. 92.2% ± 3.7%), smaller average segmental error (0.49% ± 4.35% vs. −6.11% ± 8.06%), and reduced absolute error (3.31% ± 2.87% vs. 7.96% ± 6.23%). Visual inspection of polar maps confirmed a substantial reduction of attenuation artifacts, though performance varied across subjects due to differing attenuation and uptake patterns [55].

Wang et al. (2020) describe the advancements in ML techniques, from dictionary learning and random forests to the newest designs based on convolutional neural networks. Two general approaches for use in PET attenuation correction are examined: There are two main methods for producing AC PET from non-AC PET or MR: 1) making synthetic CT and 2) converting non-AC PET to AC PET directly. Here, take a look at some of the latest studies on DL and how it may raise the bar for low-count PET reconstruction compared to traditional ML approaches [56].

There have been significant advancements in attenuation correction (AC) for PET and SPECT imaging; yet, there are still certain areas where research is lacking. Although methods based on deep learning, such as direct and indirect AC techniques, have demonstrated improved accuracy, artifact reduction, and robustness compared to conventional techniques, challenges persist in generalizability across different scanners, tracers, and patient populations. Most studies focus on cardiac or brain imaging, leaving limited exploration of whole-body or low-dose applications. Furthermore, the lack of large-scale multimodal datasets, clinically verified standards, and standardised assessment criteria prevents consistent comparison and implementation of AI-based AC approaches in normal clinical practice. Furthermore, integration of hardware innovations with AI-driven software solutions, as well as the interpretability and explainability of DL models, remain underexplored areas that are critical for regulatory approval and widespread clinical acceptance.

TABLE VIII. COMPARATIVE OVERVIEW OF ATTENUATION CORRECTION METHODS IN SPECT AND PET IMAGING

Study	Modality / Target	AC Method	Approach Type	Dataset / Sample	Key Findings / Performance	Clinical / Preclinical Use
Kawakubo et al. (2024)	Myocardial perfusion SPECT	SPECTSPT	PET-supervised DL	Stress/rest cardiac SPECT	Corrected inferior wall attenuation; outperformed conventional SPECT; practical low-cost improvement	Standalone SPECT MPI
Bouchareb et al. (2024)	SPECT & SPECT/CT	N/A	Hardware/software review	Review	Semiconductor detectors (CZT), new collimators, resolution recovery reconstruction; shorter scan times, improved image quality	Clinical cardiac imaging
Chen & Liu (2023)	SPECT / PET	Deep-learning AC	Direct & indirect DL-based AC	Review	Indirect: neural networks generate μ-maps; Direct: predict AC images	General SPECT & PET AC

					from NAC directly; DL AC ≥ conventional AC	
Du et al. (2023)	Brain SPECT (99mTc-TRODAT-1)	DL-based AC vs Chang-AC	Direct & indirect DL AC, cross/ensemble training	260 patients, 2 scanners	DL AC outperformed Chang-AC; DL-ACμ best; scanner-specific training superior	Brain SPECT, dopaminergic imaging
Mostafapour et al. (2022)	MPI-SPECT	ResNet & U-Net	Direct DL AC	99 patients, CT-AC reference	ME ResNet: −6.99 ± 16.72, U-Net: −4.41 ± 11.8; SSI ≈0.99; TPD close to CT-AC	Myocardial perfusion SPECT
Omidvari et al. (2022)	Total-body PET	Lutetium background AC	Monte Carlo simulation	3D XCAT phantom, uEXPLORER PET	Quantification within ±10% for 20-min scan; ultralow-dose feasible; scan duration and angle affect quantification	Preclinical / low-dose PET
Yang et al. (2021)	Cardiac SPECT	Direct DL AC (SPECTDL)	CNN-based direct AC	100 patients	Segmental errors reduced: −6.11 → 0.49%; voxel correlation ↑; attenuation artifacts reduced	Cardiac SPECT
Wang et al. (2020)	PET	ML / DL-based AC	Synthetic CT or direct AC	Review	ML (RF, dictionary) → CNN; DL advantages in low-count PET; direct or synthetic CT approaches	PET attenuation correction

XV. Conclusion and Future Direction

The evolution of nuclear medicine has been driven by the need for higher image fidelity, accurate quantification, and improved clinical confidence, with attenuation correction (AC) playing a pivotal role in this progress. From early uniform attenuation models to advanced CT- and MR-based μ-maps, AC techniques have transformed PET and SPECT imaging by reducing artifacts, improving contrast, and enabling reliable tracer quantification. Despite these advancements, challenges persist, including variations in scanner-specific implementations, increased radiation dose in CT-based correction, and the inherent limitations of MR-based AC in differentiating tissue types such as bone and air. Recent developments in AI and DL have opened new possibilities for generating synthetic CT images, estimating scatter more accurately, and automating correction workflows. Looking ahead, research efforts should prioritize robust validation of AI-driven methods across diverse populations, harmonization of AC techniques for cross-centre reproducibility, and the design of adaptive protocols that account for individual anatomical and physiological differences. Future directions also include closer integration of multimodal imaging data, development of low-dose and faster correction strategies, and expansion of clinical studies to confirm the impact of advanced AC on treatment planning and patient outcomes. Ultimately, by uniting hybrid imaging with computational intelligence, attenuation

correction will continue to advance the precision, efficiency, and personalization of nuclear medicine.

REFERENCES

[1] A. Könik, J. A. O'Donoghue, R. L. Wahl, M. M. Graham, and A. D. Van den Abbeele, "Theranostics: The Role of Quantitative Nuclear Medicine Imaging," 2021. doi: 10.1016/j.semradonc.2020.07.003.

[2] Y. Li *et al.*, "CT-less attenuation correction for long axial field-of-view (LAFOV) PET/CT: whole-body and total-body 18F-FDG PET on uMI Panorama GS," *J. Nucl. Med.*, vol. 65, no. 2, 2024.

[3] M. T. Madsen, "Recent advances in SPECT imaging," *J. Nucl. Med.*, vol. 48, no. 4, pp. 661–673, 2007, doi: 10.2967/jnumed.106.032680.

[4] Y. Seo, C. Mari, and B. H. Hasegawa, "Technological Development and Advances in Single-Photon Emission Computed Tomography/Computed Tomography," 2008. doi: 10.1053/j.semnuclmed.2008.01.001.

[5] E. Skoura, "Depicting medullary thyroid cancer recurrence: The past and the future of nuclear medicine imaging," 2013. doi: 10.5812/ijem.8156.

[6] S. Pandya, "A Machine and Deep Learning Framework for Robust Health Insurance Fraud Detection and Prevention," *Int. J. Adv. Res. Sci. Commun. Technol.*, Jul. 2023, doi: 10.48175/IJARSCT-14000U.

[7] G. Krokos, J. MacKewn, J. Dunn, and P. Marsden, "A review of PET attenuation correction methods for PET-MR," 2023. doi: 10.1186/s40658-023-00569-0.

[8] A. S. Lundervold and A. Lundervold, "An overview of deep learning in medical imaging focusing on MRI," 2019. doi: 10.1016/j.zemedi.2018.11.002.

[9] M. Hu, J. Zhang, L. Matkovic, T. Liu, and X. Yang, "Reinforcement learning in medical image analysis: Concepts, applications, challenges, and future directions," 2023. doi: 10.1002/acm2.13898.

[10] S. Pandya, "A Machine Learning Framework for Enhanced Depression Detection in Mental Health Care Setting," *Int. J. Sci. Res. Sci. Eng. Technol.*, vol. 10, no. 5, Oct. 2023, doi: 10.32628/IJSRSET2358715.

[11] K. C. Ma *et al.*, "Deep learning-based whole-body PSMA PET/CT attenuation correction utilizing Pix-2-Pix GAN," *Oncotarget*, vol. 15, pp. 288–300, 2024, doi: 10.18632/oncotarget.28583.

[12] W. Zhu, H. Jiang, E. Wang, Y. Hou, L. Xian, and J. Debnath, "X-ray image global enhancement algorithm in medical image classification," *Discret. Contin. Dyn. Syst. - S*, vol. 12, no. 4&5, pp. 1297–1309, 2019, doi: 10.3934/dcdss.2019089.

[13] M. Bisgaard *et al.*, "Exploring radiographers' experience with mobile X-ray of patients in their homes," *Radiography*, 2022, doi: 10.1016/j.radi.2021.08.008.

[14] S. Izadi *et al.*, "Enhanced direct joint attenuation and scatter correction ofac whole-body PET images via context-aware deep networks," *Z. Med. Phys.*, 2024, doi: 10.1016/j.zemedi.2024.01.002.

[15] W. Li, L. Fang, and J. Li, "Exposure Doses to Technologists Working in 7 PET/CT Departments," *Dose-Response*, 2020, doi: 10.1177/1559325820938288.

[16] M. A. Park, V. G. Zaha, R. D. Badawi, and S. L. Bowen, "Supplemental Transmission Aided Attenuation Correction for Quantitative Cardiac PET," *IEEE Trans. Med. Imaging*, 2024, doi: 10.1109/TMI.2023.3330668.

[17] V. K. Singh, D. Pathak, and P. Gupta, "Integrating Artificial Intelligence and Machine Learning into Healthcare ERP Systems: A Framework for Oracle Cloud and Beyond," *ESP J. Eng. Technol. Adv.*, vol. 3, no. 2, pp. 171–178, 2023, doi: 10.56472/25832646/JETA-V3I6P114.

[18] R. G. W. Lambert *et al.*, "Defining active sacroiliitis on MRI for classification of axial spondyloarthritis: Update by the ASAS MRI working group," *Ann. Rheum. Dis.*, 2016, doi: 10.1136/annrheumdis-2015-208642.

[19] Z. T. Al-Sharify, T. A. Al-Sharify, N. T. Al-Sharify, and H. Y. Naser, "A critical review on medical imaging techniques (CT and PET

scans) in the medical field," in *IOP Conference Series: Materials Science and Engineering*, 2020. doi: 10.1088/1757-899X/870/1/012043.

[20] Y. Seo, K. H. Wong, M. Sun, B. L. Franc, R. A. Hawkins, and B. H. Hasegawa, "Correction of photon attenuation and collimator response for a body-contouring SPECT/CT imaging system," *J. Nucl. Med.*, 2005.

[21] N. Zamani-Siahkali *et al.*, "SPECT/CT, PET/CT, and PET/MRI for Response Assessment of Bone Metastases," 2024. doi: 10.1053/j.semnuclmed.2023.11.005.

[22] B. B. Chin, Y. Nakamoto, D. L. Kraitchman, L. Marshall, and R. Wahl, "PET-CT Evaluation of 2-Deoxy-2-[18F]Fluoro-D-Glucose Myocardial Uptake: Effect of Respiratory Motion," *Mol. Imaging Biol.*, vol. 5, no. 2, pp. 57–64, 2003, doi: https://doi.org/10.1016/S1536-1632(03)00044-1.

[23] P. E. Kinahan and J. W. Fletcher, "Positron emission tomography-computed tomography standardized uptake values in clinical practice and assessing response to therapy," *Semin. Ultrasound, CT MRI*, 2010, doi: 10.1053/j.sult.2010.10.001.

[24] P. E. Kinahan, B. H. Hasegawa, and T. Beyer, "X-ray-based attenuation correction for positron emission tomography/computed tomography scanners," *Semin. Nucl. Med.*, 2003, doi: 10.1053/snuc.2003.127307.

[25] D. L. Chen and P. E. Kinahan, "Multimodality molecular imaging of the lung," 2010. doi: 10.1002/jmri.22385.

[26] V. Verma, "Improving Product Recommendations in Retail with Hybrid Collaborative Filtering and LSTM Varun Verma Independent Researcher," *Int. J. Eng. Sci. Math.*, vol. 10, no. 8, pp. 113–128, 2021.

[27] S. Y. Chun, J. A. Fessler, and Y. K. Dewaraja, "Correction for Collimator-Detector Response in SPECT Using Point Spread Function Template," *IEEE Trans. Med. Imaging*, vol. 32, no. 2, pp. 295–305, Feb. 2013, doi: 10.1109/TMI.2012.2225441.

[28] V. Thakran, "A Review of 3D printing methods for pharmaceutical manufacturing : Technologies and applications," *Int. J. Sci. Res. Arch.*, vol. 04, no. 01, pp. 250–261, 2021.

[29] P. Zanzonico, "Positron Emission Tomography: A Review of Basic Principles, Scanner Design and Performance, and Current Systems," *Semin. Nucl. Med.*, 2004, doi: 10.1053/j.semnuclmed.2003.12.002.

[30] H. Choi, "Deep Learning in Nuclear Medicine and Molecular Imaging: Current Perspectives and Future Directions," 2018. doi: 10.1007/s13139-017-0504-7.

[31] S. W., "SPECT image reconstruction by deep learning using a two-step training method," *J. Nucl. Med.*, 2019.

[32] C. Li *et al.*, "Recent advances in solution-processed photodetectors based on inorganic and hybrid photo-active materials," 2020. doi: 10.1039/c9nr07799e.

[33] G. K. Loudos *et al.*, "Improving spatial resolution in SPECT with the combination of PSPMT based detector and iterative reconstruction algorithms," *Comput. Med. Imaging Graph.*, 2003, doi: 10.1016/S0895-6111(02)00080-0.

[34] T. Funk, P. Després, W. C. Barber, K. S. Shah, and B. H. Hasegawa, "A multipinhole small animal SPECT system with submillimeter spatial resolution," *Med. Phys.*, 2006, doi: 10.1118/1.2190332.

[35] M. Occhipinti *et al.*, "A compact SiPM photodetector array for SPECT applications," in *2014 IEEE Nuclear Science Symposium and Medical Imaging Conference, NSS/MIC 2014*, 2016. doi: 10.1109/NSSMIC.2014.7430864.

[36] F. Caobelli *et al.*, "IQ SPECT allows a significant reduction in administered dose and acquisition time for myocardial perfusion imaging: Evidence from a phantom study," *J. Nucl. Med.*, 2014, doi: 10.2967/jnumed.114.143560.

[37] T. Winuprasith, P. Koirala, D. J. McClements, and P. Khomein, "Emulsion Technology in Nuclear Medicine: Targeted Radionuclide Therapies, Radiosensitizers, and Imaging Agents," 2023. doi: 10.2147/IJN.S416737.

[38] A. Zatcepin and S. I. Ziegler, "Detectors in

positron emission tomography," 2023. doi: 10.1016/j.zemedi.2022.08.004.

[39] J. Lau, E. Rousseau, D. Kwon, K. S. Lin, F. Bénard, and X. Chen, "Insight into the development of PET radiopharmaceuticals for oncology," 2020. doi: 10.3390/cancers12051312.

[40] B. D. Wright and S. E. Lapi, "Designing the magic bullet? the advancement of immuno-PET into clinical use," *J. Nucl. Med.*, 2013, doi: 10.2967/jnumed.113.126086.

[41] S. Minoshima *et al.*, "SNMMI procedure standard/EANM practice guideline for amyloid PET imaging of the brain 1.0," *J. Nucl. Med.*, 2016, doi: 10.2967/jnumed.116.174615.

[42] R. Harada, N. Okamura, S. Furumoto, and K. Yanai, "Imaging protein misfolding in the brain using β-sheet ligands," 2018. doi: 10.3389/fnins.2018.00585.

[43] Y. Li, W. Zhang, H. Wu, and G. Liu, "Advanced tracers in PET imaging of cardiovascular disease," 2014. doi: 10.1155/2014/504532.

[44] S. Auletta, M. Varani, R. Horvat, F. Galli, A. Signore, and S. Hess, "PET radiopharmaceuticals for specific bacteria imaging: A systematic review," 2019. doi: 10.3390/jcm8020197.

[45] M. P. Kung *et al.*, "Radioiodinated styrylbenzene derivatives as potential SPECT imaging agents for amyloid plaque detection in Alzheimer's disease," *J. Mol. Neurosci.*, 2002, doi: 10.1007/s12031-002-0003-9.

[46] G. Crișan, N. S. Moldovean-Cioroianu, D.-G. Timaru, G. Andrieș, C. Căinap, and V. Chiș, "Radiopharmaceuticals for PET and SPECT Imaging: A Literature Review over the Last Decade," *Int. J. Mol. Sci.*, vol. 23, no. 9, p. 5023, Apr. 2022, doi: 10.3390/ijms23095023.

[47] F. F. Alqahtani, "SPECT/CT and PET/CT, related radiopharmaceuticals, and areas of application and comparison," 2023. doi: 10.1016/j.jsps.2022.12.013.

[48] K. Vats, A. Chakraborty, S. Rakshit, A. Damle, H. D. Sarma, and D. Satpati, "[99mTc]Tc-HYNIC-RM2: A potential SPECT probe targeting GRPR expression in prostate cancers," *Nucl. Med. Biol.*, 2023, doi: 10.1016/j.nucmedbio.2023.108331.

[49] M. Kawakubo *et al.*, "Deep learning approach using SPECT-to-PET translation for attenuation correction in CT-less myocardial perfusion SPECT imaging," *Ann. Nucl. Med.*, 2024, doi: 10.1007/s12149-023-01889-y.

[50] Y. Bouchareb *et al.*, "Technological Advances in SPECT and SPECT/CT Imaging," *Diagnostics*, vol. 14, no. 13, 2024, doi: 10.3390/diagnostics14131431.

[51] X. Chen and C. Liu, "Deep-learning-based methods of attenuation correction for SPECT and PET," *J. Nucl. Cardiol.*, 2023, doi: 10.1007/s12350-022-03007-3.

[52] Y. Du *et al.*, "Generative adversarial network-based attenuation correction for 99mTc-TRODAT-1 brain SPECT," *Front. Med.*, 2023, doi: 10.3389/fmed.2023.1171118.

[53] S. Mostafapour *et al.*, "Deep learning-guided attenuation correction in the image domain for myocardial perfusion SPECT imaging," *J. Comput. Des. Eng.*, 2022, doi: 10.1093/jcde/qwac008.

[54] N. Omidvari *et al.*, "Lutetium background radiation in total-body PET—A simulation study on opportunities and challenges in PET attenuation correction," *Front. Nucl. Med.*, 2022, doi: 10.3389/fnume.2022.963067.

[55] J. Yang *et al.*, "Direct attenuation correction using deep learning for cardiac SPECT: A feasibility study," 2021. doi: 10.2967/jnumed.120.256396.

[56] T. Wang *et al.*, "Machine learning in quantitative PET: A review of attenuation correction and low-count image reconstruction methods," 2020. doi: 10.1016/j.ejmp.2020.07.028.